Preface

This master's thesis was written in 2022 for the degree of electromechanical engineering at the faculty of engineering technology. This joint programme is provided by both UHasselt and KULeuven. The research was performed at Energyville in Genk, Belgium. This research collaboration handles many advanced topic, all related to durable and intelligent energy systems.

For my master's thesis, I was able to set up and execute experiments, while being part of the thin film PV research teams. In addition to honing my research skills, I learned communication skills by contributing to the ongoing efforts at Energyville. I chose thin film as my subject because it directly aligns with my ambition to develop renewable energy sources and working with solar technology seemed to be a fitting introduction.

First of all, I would like to thank Prof. dr. ir. Guy Brammertz and Prof. dr. Bart Vermang, my promotors, for the wonderful guidance throughout the whole proces. They have always answered to my questions with care and I have welcomed any feedback they provided. Their help in the research itself was indispensible. Also, I would like to thank Tim Oris, a member of the thin film PV team at Energyville, for providing much advice and support. Especially his familiarity with the sputtering process taught me how to operate the tool, in addition to him aiding in the design of experiments.

Frederik Vanherf

Maasmechelen 2022

Contents

List of Tables

List of Figures

Abstract

Energyville conducts research in thin film photovoltaics, with a focus on , among others, Copper Indium Gallium Selenide (CIGS) cells. The top two layers of CIGS solar cell are Indium tin oxide (ITO) and zinc oxide (ZnO). The main goal is to optimize the optoelectrical properties of these top layers and to reduce the induced sputtering damage to underlying layers, so as to increase the solar performance.

The window layers were deposited with a linear RF sputtering system. The effects of working pressure, annealing, substrate carrier speed, CdS waiting times and sputtering power on the optoelectrical properties and deposition mechanism were analyzed.

An elevated working pressure caused a small decrease in ITO resistivity and a significant increase of ZnO resistivity, while improving the short-term stability of solar cells. This was attributed to a reduced impact energy, resulting in less defects. A lower carrier speed had no significant effect on the optoelectrical properties and worsened cell performance. Sealing the samples vacuum immediately after CdS reaction allowed for better cell performance. A lower sputtering power for the initial ZnO layer caused a significant increase for the fill factor, which resulted in a 2.2% increase of the conversion efficiency for co-evaporated CIGS. The quality of the window layers was improved slightly, with an ITO resistivity around $5.82 \cdot 10^{-4} \Omega cm$ ($2.03 \cdot 10^{-4} \Omega cm$ after O2 annealing) and transmittance of 87% at 500 nm. More efficient and less deteriorating CIGS solar cells were realised.

Abstract in Dutch

Energyville verricht onderzoek op het gebied van dunne-film fotovoltaïsche cellen, waarbij Copper Indium Gallium Selenide (CIGS) één van de huidige onderwerpen is. Indiumtinoxide (ITO) en zinkoxide (ZnO) films, de toplagen van CIGS-zonnecellen, werden gedeponeerd met een lineair RF-sputtersysteem.

De effecten van de werkdruk, gloeien, houdersnelheid, CdS-wachttijden en sputtervermogen op de opto-elektrische eigenschappen en het depositiemechanisme werden geanalyseerd. Dit werd gedaan om de geleidbaarheid en de transmissie van deze vensterlagen te optimaliseren en de schade aan de onderliggende lagen, geïnduceerd door het sputteren, te verminderen.

Een verhoogde werkdruk veroorzaakte een kleine afname van de weerstand van ITO en een aanzienlijke toename van de weerstand van ZnO, terwijl de korte termijn stabiliteit van de zonnecellen werd verbeterd. Dit werd toegekend aan een verminderde impactenergie, wat resulteerde in minder defecten. Een lagere houdersnelheid, samen met minder passen, had geen significant effect op de opto-elektrische eigenschappen en verslechterde de zonnecelprestaties. De vacuümverzegeling van de monsters, onmiddellijk na de CdS-reactie, zorgde voor betere celprestaties. Een lager sputtervermogen voor de initiële ZnO-laag veroorzaakte een significante toename van de vulfactor, wat resulteerde in een toename van het omzettingsrendement met 2,2 % voor co-evaporated CIGS. De conclusie is dat de kwaliteit van de vensterlagen redelijk hoog is, met een ITO-weerstand rond $5.82 \cdot 10^{-4} \Omega cm$ ($2.03 \cdot 10^{-4} \Omega cm$ na O2-gloeien) en een transmissie van 87% bij 500 nm. Efficiëntere en minder degraderende CIGS-zonnecellen werden gerealiseerd.

Chapter 1

Introduction

1.1   Context

The master's thesis was performed at Energyville 2 in Genk, which is a coalition of IMEC, UHasselt, KULeuven and VITO. Energyville 2 researches and develops innovations in photovoltaic (PV) and battery applications. One of these PV innovations are Thin Film Photovoltaics (TFPV) which can be implemented in flexible or semitransparent settings. Additionally, ongoing projects are looking into tandem modules, where high band gap TFPV function as top cells and are combined with low band gap cells underneath. The tandem modules can reduce the thermalization losses and increase the energy conversion efficiency.

There are several types of TFPV, with Cu2(In,Ga)Se2 (CIGS) cells[1] being the focus of this master's thesis. These specific solar cells consist of several layers deposited on top of a glass substrate. From the bottom up they are Molybdenum (as the back contact), CIGS (as the absorber), CdS (as the buffer layer), ZnO (as a short circuit barrier) and finally the Transparent Conductive Oxide (TCO), which functions as the front contact and the window layer. Fig. 1.1 shows the composing layers of a CIGS solar cell. The window layer consists of a TCO, which serves to transmit the incoming light and conduct the generated electrons. In Energyville 2, mainly Indium Tin Oxide (ITO) in combination with ZnO is used for this top layer. Additionally, a silver grid is added to complete the solar cell. In some integrated modules, this layered structure is topped off by another glass plane.

1.2   Research question

The window layer of the CIGS cell is essential to the collection of charges generated in the absorber layer. Therefore, the collected carriers have to be able to pass through the TCO layer easily. This can be achieved when the sheet resistance of the section is low. Equally important is that the window layer is able to transmit a broad spectrum of the incoming light. Therefore, a high transparency and low reflectivity are desirable for the TCO. The conductivity and the transmissivity are the primary properties that define the performance of the window layer.

The ITO and ZnO layers must be on a nanometer scale and are therefore deposited using a

---

[1]CIGS indicates which elements are used in the absorption layer of the solar cell: copper, indium, gallium and selenium
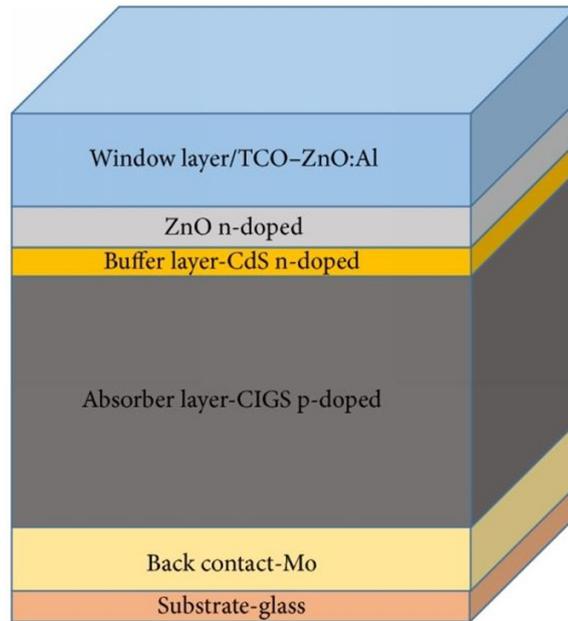
Figure 1.1: Layer composition of CIGS solar cells [1]

linear reactive sputtering tool. This process is controlled by a variety of parameters such as the power of the tool, the geometry and composition of the targets, the pressure inside the sputter chamber, the oxygen and argon flow rates and the sputtering time (which correlates to the speed of the holder and the number of passes). It has been observed that changing one of these parameters influences some of the other parameters. Because of this complexity, optimizing the sputtering process requires many trials . The quality of the deposition directly translates into the performance of the window layer. There have been preceding optimization efforts performed by the researchers at Energyville 2. These efforts have resulted in a number of baseline recipes for the sputtering process and have provided a dataset of measurements. However, a persisting demand for optimizing the window layer remains. There are still some effects of parameters that have not been thoroughly explored.

Taking the layer properties and sputtering process into account, the primary research question can be formulated as follows: How can the electrical and optical properties of the TCO be improved by optimizing the parameters of the sputtering process? The optimization of the properties of the window layer should contribute to the overall efficiency of the CIGS solar cell. Additionally, observations show that some materials used in CIGS solar cells might degrade over time. A stability analysis of the TCO might be necessary. Finally, sputtering can cause damage to the underlying layers. Therefore, the necessary optimization also includes the deposition procedure and corresponding parameters such as thickness and power. As it stands , the performance still has potential to improve and the window layer can be considered to be one of the many limiting factors in the development of TFPV.

1.3 Objectives

The main objective of this master thesis is ultimately to increase the efficiency of the CIGS solar cells, relative to the existing baseline samples produced in Energyville 2 or in comparison with samples from other research facilities. However, this is a complex objective since the solar cell is comprised of many layers, all of which contribute to the achieved efficiency. Therefore, the success of the TCO layer, being on top of the solar cell, is heavily influenced by the quality of the underlying depositions. In an initial phase, the optimization of the optical and electrical properties of the TCO will be independent of the other layers, by depositing on just a glass substrate. A later phase enables the integration of the window layer into the CIGS stack, which also allows the study of the damage caused by the sputtering process. Furthermore, after some time, the stability of the integrated materials can be verified by follow up characterization.

In both phases, the aim is to understand which parameters contribute in a significant way to the properties of the TCO. By analyzing the effect of changing the untested parameters, a better performance of the TCO could be achieved. In particular, the pressure of the plasma can still be altered to potentially improve the process. Meanwhile, the other parameters have to be monitored to check for dependencies and possibly altered to stabilize the process.

1.4 Materials and methods

The materials used mostly revolve around TCOs such as ITO and ZnO. They are relatively common in industrial applications. ITO is known for its intrinsically high conductivity, while being a transparent oxide (when applied in thin layers). ZnO on the other hand has a significantly higher resistivity and can be interpreted as an insulating layer. These TCOs are the targets in the sputtering tool and form a massive bulk material. Since these materials are oxides, they have a large DC impedance and therefore, RF sputtering is necessary. Additionally, sputtering uses oxygen and argon to create a plasma in a low-pressure chamber. Mainly soda lime glass is used as the substrate of the samples.

The research can be divided into two main parts, being the processing of the samples, inspired by a design of experiments, and the characterization of the properties. In the first part, there are several steps which have to be executed in a specific order. Firstly, the glass substrate has to be cleaned to ensure no impurities influence the deposition. Secondly, the samples have to be placed correctly into the holder of the sputtering tool. Thirdly, the right recipe has to be created and selected to allow for alterations in the sputtering process. Fourthly, after removal from the holder, the samples have to be checked for defects before being characterized.

The characterization of the electrical and optical properties of the TCO also consists of several steps which are as following. Firstly, a profilometer is used to measure the thickness of the deposited layer. Secondly, a four point probe measures the sheet resistance of the TCO. Thirdly, a Hall-effect measuring tool enables a deeper analysis of the carrier mobility and resistivity. For this third characterization, part of the sample has to be cut to a smaller format (1 x 1 cm). Fourthly, the remaining sample undergoes transmissivity and reflectivity testing with a spectral response instrument. As a final step, the layers will also be deposited on CIGS absorbers and the efficiencies of the cells will be improved with respect to the developed recipes.

1.5 Preview

In the following chapter, a literature study will be performed with the goal to describe PV performance and basic modeling. Additionally, the literature study will summarize preceding publications regarding the optimization of the window layers.

The chapters thereafter will describe the experimental setup and the obtained results, corresponding to each parameter experiment. Finally, these results will be analyzed and interpreted to formulate fitting explanations. These findings will then be summarized in the conclusion.

Chapter 2

Literature study

2.1 Introduction

As solar power becomes not only more prominent, but also more necessary, continuous efforts have to be undertaken to research novel techniques and improve performance. CIGS solar cells are an alternative to conventional crystalline silicon cells. The thin film CIGS has many advantages over silicon. Firstly, they use less material, significantly reducing the cost of modules. Secondly, because of the small thickness, CIGS can be deposited on flexible substrates. Thirdly, they possess a direct-bandgap material which can absorb a large portion of the solar emission spectrum. Fourthly, CIGS cells can be integrated into tandem cells, which can increase the energy conversion efficiency.

The focus of this thesis is the deposition of the window layers of the solar cells. In this literature study, the most notable aspects of TCO's will be discussed. First, a concise overview of the most important photovoltaic terms and definitions is given. Subsequently, the different materials, the implementation of layering and the deposition techniques will be discussed, to indicate the many possibilities when it comes to TCO's. Furthermore, the sputtering process will be analyzed, since it is the main deposition method for creating the window layers in Energyville. The sputtering process consists of many parameters that can be altered to optimize the properties of the material. Finally, the conclusion contains the most valuable understandings .

2.2 Photovoltaic terms and definitions

The performance of photovoltaics can be described with an equivalent model of the electronic structure. This model consists of an ideal current source , which delivers the short circuit current (I_{sc}), and two diodes in forward bias. The first diode represents the recombination current in the quasi-neutral regions, while diode 2 represents recombination in the depletion region [11]. However, this ideal model does not take into condsideration parasitic resistance effects. Therefore, to create a realistic model, a shunt resistance (R_{sh}) is placed in parallel, which limits the open-circuit voltage (V_{oc}). In series with the aforementioned components is the series resistance (R_s), which in turn reduces the short-circuit current. When incoming light powers the cell, the voltage and current are measured and the I-V characteristic can be obtained. Figure 2.1 shows an example of such a curve, for a silicon cell with an active area of 100 cm^2 [11]. It shows the

open-circuit voltage, the short-circuit current and the maximum power point.
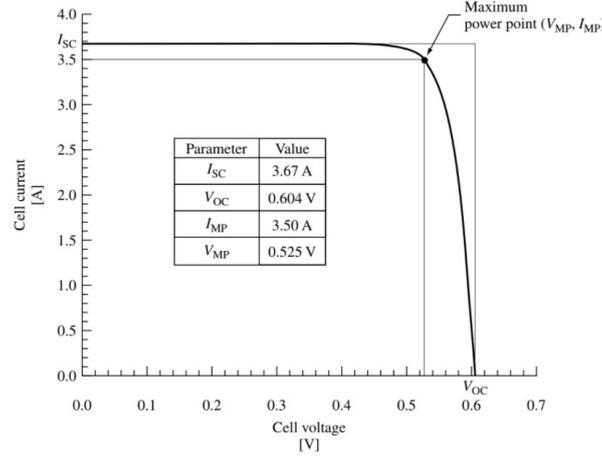
Figure 2.1: I-V characteristic of silicon solar cell [2]

The variables derived from the I-V curve can be used to describe the performance of a solar cell. The maximum power point can be compared to the rectangle defined by I_{sc} and V_{oc}. This results in the fill factor FF, which is a measure of the squareness of the I-V characteristic and is always less then one. It is the ratio of the areas of the two rectangles:

$$FF = \frac{P_{MP}}{V_{oc} \cdot I_{sc}} = \frac{V_{MP} \cdot I_{MP}}{V_{oc} \cdot I_{sc}} \tag{2.1}$$

This leads to arguably the most important figure of merit, being the power conversion efficiency η. It can be derived using the previously introduced I_{sc}, V_{oc}, FF and the incident solar power:

$$\eta = \frac{P_{MP}}{P_{in}} = FF \frac{V_{MP} \cdot I_{MP}}{V_{oc} \cdot I_{sc}} \tag{2.2}$$

Taking this formula into account, the desired properties of an efficient solar cell are known. It needs to posses a high short-circuit current, a high open-circuit voltage and a fill factor as close as possible to 1. Therefore the design of photovoltaics should aim for the minimization of recombination[1] rates throughout the device and the maximization of the absorption of photons with sufficient energy [11].

2.3 Transparent conductive oxides

2.3.1 Frequently used materials

Transparent and conducting materials are fundamental in the development of many engineering applications. These include smart flat-panel displays, touch screens, light emitting diodes and ofcourse in photovoltaic cells [12]. In PV, they are commonly chosen to be deposited as the front contact to maximize light throughput and conductivity.

---

[1]Recombination is when an electron falls from the conduction band to the valence band, thereby eliminating the valence-band hole that was created trough the absorption of light [11].

There are three main materials in this class: $SnO_2, In_2O_3 : Sn$ (ITO), and ZnO. SnO_2 requires relatively high deposition temperatures that restrict the potential in Cu(InGa)Se2 devices that cannot withstand temperatures greater than 200 to 250 °C after Cds deposition. ZnO is favorable because of its lower material costs [2]. However, intrinsic ZnO is higly resistive and is therefore regularly doped with aluminium, if it needs to serve as the front contact. Additionally, intrinsic ZnO is used as a buffer layer in between the CdS and the front contact, as will be discussed later. Apart from i-ZnO, ITO is currently used in many applications because of its desirable optoelectrical properties. It is a n-type, highly degenerative TCO with a wide band gap, a relatively low resistivity and a high transmittance in the visible range [13].

Among this list of TCO's with improved properties for demanding applications, indium tin oxide (ITO) is commonly used in electronic devices because of its excellent electrical and optical properties [12].

There exist alternatives to the most common groups of TCO's, such as FTO, AZO, GZO and many more. Even though they have not yet been popularized, they seem to provide some advantages. However, they might not be suitable for every application or might not prove cost-effective.

2.3.2 Effect of layering

There has been much development regarding the possibility of stacking several different layers on top of each other to improve the desired properties of the window layers. In this paragraph, some examples are discussed. They provide an idea of how the structure of the window layers can be altered to have an impact on the performance.

One of these structures is known as $ITO/ATO/TiO_2$, where ATO stands for antimony-doped tin oxide and TiO_2 for titanium oxide. The name indicates that ITO is the first layer, followed by ATO and finished by TiO_2. In [14], it was observed that this triple layer caused not only little change in the sheet resistance, but also a significant increase of PV performance (from 4,6 % to 6,3 %). This enhanced performance was attributed to an improved adhesion and a reduction of the electron-loss, which results in a higher photovoltage and fill factor.

Another category is that of IMIs (ITO-metal-ITO) multilayers. An example being ITO/Au/ITO, which can significantly reduce the resistivity, as reported in [15]. The sheet resistance dropped from 130 Ω/sq to around 21 Ω/sq, by inserting a thin gold layer in between two ITO layers. However, this gold layer caused a decrease in transmittance from 77 to 73 %, both at 550 nm. The reduction in sheet resistance could be amplified by annealing the layer post-deposition, resulting in a sheet resistance of 8 Ω/sq, and increasing the transmittance to 82 % at 550 nm.There are alternatives for the expensive gold layer, such as in [16], where a 10-mm Ag intermediate layer is introduced. It allowed for the resistivity to be lowered by a factor of four, while not affecting the optical transmittance.

Finally, there exist techniques to improve the transmittance and conductivity of a single material by depositing in two steps. An example of this has been developed in [17], where a primary thin seed ITO layer (40 nm) with a dense surface is overlapped by a thick secondary ITO layer (160 nm). The seed layer is deposited with a gas flow only containing argon and no oxygen, at a working pressure of 0,3 Pa. For the thick bulk layer, 2 sscm of oxygen is added, while the working pressure was increased to 0,5 Pa. The two-step deposition results in a lower resistivity (19,7

Ω/sq) and a higher transmittance (83%)in the visible spectral range. The proposed explanation is that the dense layer in the first step promotes the further growth of the ITO. Additionally, the incorporation of oxygen in the second step is suspected to provide the improved transmittance.

For all multilayer TCO structures, the connection of each layer to not only the other layers, but also to the preceding layers of the solar cell can cause defects. Interfaces between two dissimilar materials have a high concentration of defects due to the abrupt termination of the crystal lattice [11]. If the transition between subsequent layers is too abrupt, the created interface causes a drop in transmittance, in addition to recombination losses.

2.3.3   Deposition techniques

There exists a large variety of techniques for depositing TCO's, each having its own advantages and drawbacks. One of the most commonly used techniques is sputtering, of which there are many types. For the case of ITO and ZnO, RF sputtering is a familiar and reliable option. Additionally, it is considered to be a flexible and scalable technique, accessible for large area depositions. For sputtering, the target consists of the desired metal-oxide and is subjected to a plasma consisting of argon and other incoming gasses (mainly oxygen). It is a rather complex process in comparison with direct deposition and relies on the generation, absorption and reaction of the reactive species (atoms or ions) [18]. The sputtering mechanism will be explained in the following section, since the complexity of this process requires a detailed description.

Another technique that is used in many applications is thermal evaporation [19], which is a type of direct deposition, widely used in vacuum coating. In essence, it is achieved by resistive heating of a filament or crucible or by electron beam heating. The evaporant is heated to a temperature such that the vapor pressure becomes appreciable and atoms or molecules are lost from the surface and subsequently condense on the substrate. Deposition is performed in a good vacuum to maintain the composition of the evaporant. However, it is also possible to add a reactive gas to create a compound material.

TCO's such as ITO can also be deposited by chemical vapour deposition (CVD) [20]. However, to obtain such a thin film, a precursor material is needed, which has to be volatile but thermally stable. An example of such a precursor material is tin(IV)chloride, which serves as the tin dopant in the creation of ITO layers starting from indium 2-ethylhexanoate. The layer is deposited on a heated substrated via a chemical reaction of gas-phase precursors. In [20], this technique resulted in ITO films with a resistivity of $2,9 \cdot 10^{-4}\Omega cm$ and a transmittance more than 80 % at 550 nm.

A final deposition technique that has gained popularity over the years is pulsed laser deposition (PLD) [21]. The deposition is realised by focusing a high-power laser beam inside a vacuum chamber which hits the target material. A plasma plume, containing the ablated target atoms, is created and hits the substrate, promoting the crystalline growth of the thin film. With PLD, an atomic layer precision is possible. It allows for high quality ITO films with a resistivity of $3,3 \cdot 10^{-4}\Omega cm$ and a transmittance above 90 %, at a pressure of 2.0 Pa.

2.4 Sputtering process types

2.4.1 Sputtering mechanism

The lab of Energyville possesses a large area sputtering tool which can deposit using either a Direct-Current (DC) or a Radio Frequency (RF) power source. In prior art, both source types are commonly used for the sputtering of window layers. It is a rather complex process, with many defining parameters, including both the plasma conditions and the geometry of the target and substrate. Figure 2.2 provides a diagram of the sputtering process.

To get a basic understanding of the fundamentals, the mechanisms that occur during the sputtering process will now be discussed. After reaching vacuum, the sputtering chamber is filled with a high purity inert process gas, which is usually Argon due to its relative mass and ability to convey kinetic energy upon impact. Typical sputter pressures can range from 0,5 mTorr to 100 mTorr.

The power source runs an energetic field through an inert gas in a vacuum chamber which becomes ionized, due to collisions with free electrons. The target material, which functions as the cathode, is bombarded by these high energy ions, causing ions to sputter of. These target atoms are then sprayed onto the substrate. When an Argon ion recombines with an electron, a neutralized atom is formed which emits radiation. This is visible as the light that the plasma emits [3].
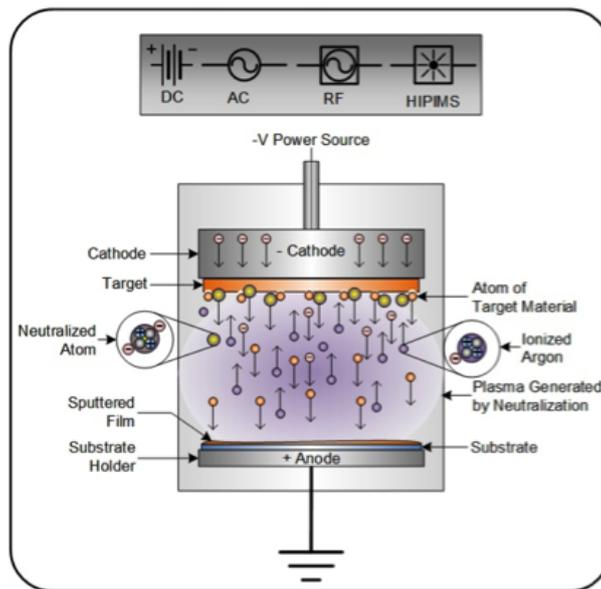
Figure 2.2: Diagram of the sputtering process [3]

It is called magnetron sputtering if the substrate rotates relative to the target. In a linear sputtering system the target moves with a constant speed back and forth, depositing in a series of passes until the desired thickness is reached.

2.4.2 DC sputtering

DC-sputtering is the most basic and inexpensive type of sputtering. Two major advantages of DC as a power source is that it is easy to control and is a low cost option. In large scale

manufacturing, DC sputtering from ceramic targets is favored since it requires simpler equipment and offers higher deposition rates [2].

In [22], where ZnO:Al films were optimized for CIGS mini-modules, it was observed that DC-sputtering causes less damage to underlying layers, due to lower ion bombardment, but result in films with a higher resistivity. The damaged could be mitigated even further by reducing the sputtering power level, thereby improving the FF.

DC-sputtering also knows some disadvantages, as it is limited when it comes to dielectric target materials [2]. DC sputtering also causes the plasma to concentrate around the target material, which is not always desirable.

2.4.3   RF sputtering

RF sputtering is a technique where an alternating electrical potential at radio frequencies is implemented. Breakdown ionisation is created by heating the electrons with a fluctuating electric field. It is a self sustained and stable sputtering process, in addition to being more suitable for poor conducting materials [23]. The alternating power source is used to avoid a charge buildup on certain types of target materials. Over time, this can cause arcing in the plasma and the spewing droplets, which creates quality control issues. With the RF potential, the target is cleaned of charge buildup with each cycle [3]. The RF AC voltage is a combination of DC and AC voltage such that it has a positive magnitude, 75% of the time.

Additionally, experimental results [23] showed that RF produced ZnO-films had a better quality than DC ZnO-films. It has been contemplated that RF excitation has a higher degree of ionisation/dissociation which leads to a higher oxidation rate at the substrate surface. This is because of the larger ratio of O to Zn that arrive at the substrate. RF discharge also leads to a more intensive ion bombardment of the growing film. The higher ion densities provide an additional energy input, which causes the surface mobility to increase, improving the film perfection.

However, RF sputtering provides a lower deposition rate and involves several important costs. Radio waves require much higher voltage to achieve similar deposition results as with direct current, which results in overheating problems.

2.5   Sputtering parameters

There are many parameters that define the sputtering process. Changing one of these parameters might inadvertently change others. Therefore, it is crucial to actively monitor the other parameters while performing experiments. Not all of these parameters have an equal effect on the properties that are being optimized. These effects, as described in existing publications, might not be reproducible with the setup used in this thesis. The sputtering tool in publications can differ a lot from the one used in Energyville. Also, it is important to note that there are many other parameters in the sputtering process, but only the ones that are possible to be altered with the tool in the lab will be discussed.

The parameters that will be studied in the next paragraphs are the gas mixture, the working

---

[2]Dielectric materials are non-conducting materials that can take on a polarized charge. Examples in a PV setting are Aluminium Oxide, Silicon Oxide and Tantalum oxide [3]

pressure, the deposition time, the addition of hydrogen and the sputtering power. Additionally, the effects of annealing and thickness variations will be discussed.

2.5.1 Gas mixture

The gas mixture is proven to be one of the dominant parameters in the sputtering process. It determines not only the composition of the deposited material, but also has a major effect on the resistivity and transmittance of the created layer. In most applications, the gas mixture consists of argon and oxygen gas. In almost all TCO manufacturing, oxygen only makes up a small fraction of the total gas flow. It mainly serves to compensate for a loss of oxygen atoms in the deposition matrix. Not all oxygen that gets sputtered off the target makes it to the substrate. Additionally, the stoichiometry of the layer can be disturbed when more metal relative to oxygen is removed from the target. Both phenomena cause oxygen vacancies to form.

The effects of the oxygen concentration on the electrooptical properties of ITO were analysed in [21]. The oxygen vacancies result in a high carrier concentration, which can reduce the resistivity of the deposited layer. This is because every oxygen vacancy creates two extra electrons in the films. Starting from 0%, a small increase of the oxygen flow leads to a reduced amount of lattice structural defects. However this initial drop in resistivity reaches a minimum and from thereon, increasing the oxygen concentration further causes the sheet resistance to rise again. This increase in oxygen starts compensating for the sputtering loss and essentially fills the oxygen vacancies, reducing the amount of extra free electrons. The initial drop and later rise can be seen in figure 2.3. This figure originates from another study [4] which observed the same trends regarding the oxygen flow. However, it also stated that control over these trends is rather difficult. Another study [5] also stated that in essence, a small increase in oxygen atoms affects the ordering of the crystal structure, because amorphous TCO's will be severely disordered with non-stoichiometry. However, further increase of oxygen concentration inversely affects the carrier concentration.
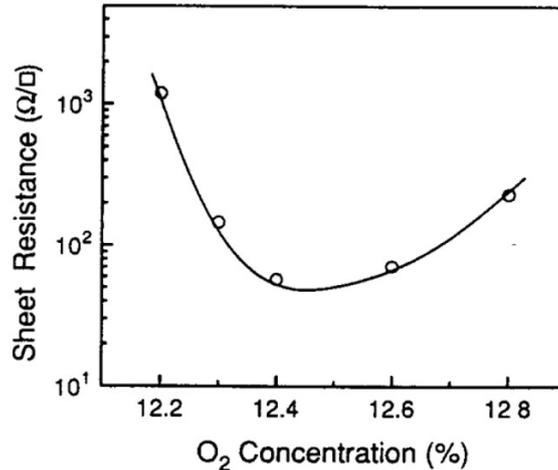
Figure 2.3: Sheet resistance in function of oxygen concentration for ITO [4]

The oxygen vacancies also affect the transmittance and the absorbance of the TCO. Optical properties mainly depend on crystal quality and carrier concentration. A higher concentration of oxygen results in the film having a lower absorption in the visible range. According to [24], this is due to the increased bands below the Fermi level and the presence of an entire second band gap. Additionally, it was observed that the optical absorption edge was blue-shifted.

23

Similar effects on resistivity and have been found in [5], where it was concluded that the increase in oxygen also caused a decrease in growth rate, which in turn caused a decrease in resistivity because of the smaller particle size. At 10% oxygen, the transmittance reached its optimum, being 85%, which was theorized to be because of the widening of the band gap of the material. The positive trend of the transmittance is illustrated in figure 2.4. In [8], it is recommended to keep the oxidation state constant, which is essential to increasing the transmittance and reducing the resistance.
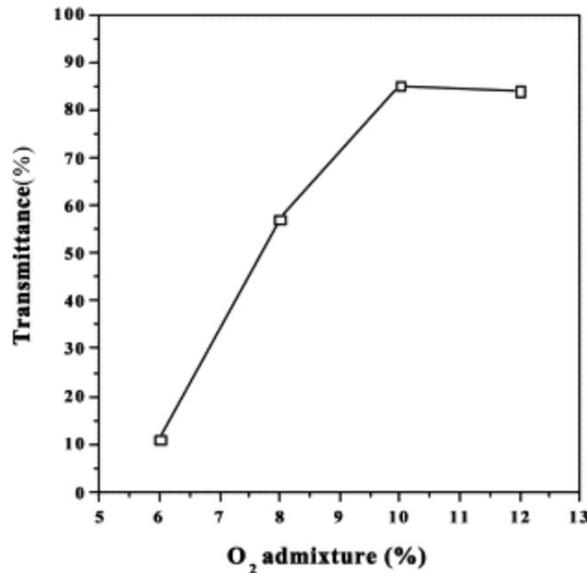
Figure 2.4: Transmittance in function of the oxygen admixture for ITO [5]

2.5.2   Working pressure

Inside the sputtering chamber, there are two types of pressure that can be identified. When the pumping down of the chamber is finished, there will always remain a residual pressure in the background, which is called the base pressure and is generally in the order of microTorrs. The lower the base pressure, the fewer residual impurities in the sputtering cavity [25]. When the sputtering starts and the gas mixture is introduced, another pressure appears, which is the working pressure. It is controlled by how much argon and oxygen gas is introduced but also how much of these is pumped out of the chamber. The working pressure varies a lot between publications (from 2 mTorr [17] to 150 mTorr [6]).

The main principal behind altering the working pressure is that it significantly reduces the excess kinetic energy of the ionised argon atoms, thereby possibly reducing the damage caused by ion bombardment. A generally accepted explanation is that the higher pressure means that there are more argon atoms in between the target and the substrate, which act as obstacles for the sputtered target atoms [9]. These metal atoms reach the growing film with less kinetic energy and create less dislocations. It results in a better adhesion of the film and can reduce its contact resistivity. However, not all publications show the same trends regarding an increase in working pressure, which will be discussed in the following paragraphs.

In a recent publication [6] the effect of the working pressure on the optoelectronic properties of ITO films prepared by high power impulse magnetron sputtering was analyzed. The resistivity of the film was measured at different working pressure, as shown in figure 2.5.
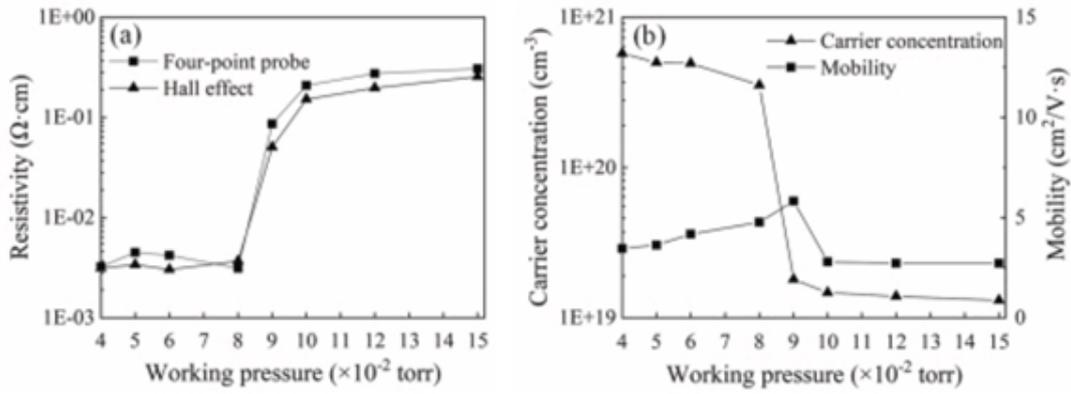
Figure 2.5: Resistivity (a), carrier concentration (b) and mobility (b) in function of working pressure for ITO [6]

The restivity seems to initially increase significantly and stagnates at higher pressures. This can be understood if also the carrier concentration and the mobility are taken into consideration, since multiplying both properties provides a possible method of determining the conductivity. Mainly the carrier concentration drops immensely at a pressure higher than 90 mTorr. This could be due to the lower kinetic energies incident to the film, which can reduce the likelihood that tin atoms are incorporated into the indium substitutional sites during growth. This effect is enhanced at room temperature and as a result, the electron carrier concentration is reduced.

However, this conclusion is debatable since there exist numerous studies, as listed in [8], that claim that the resistance decreases with a higher working pressure. Figure 2.6 shows the resistivity, mobility and carrier concentration in function of the pressure.
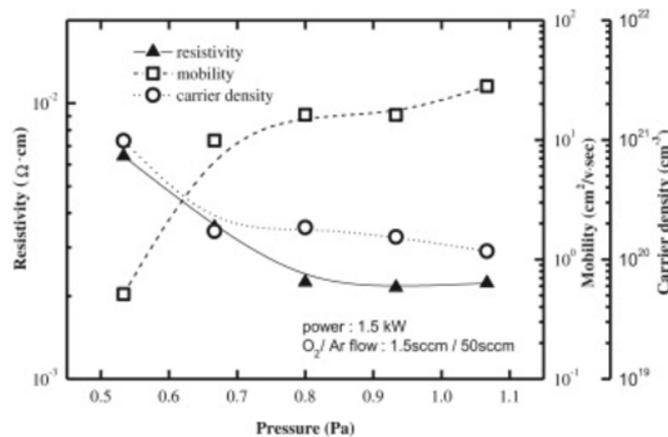
Figure 2.6: Resistivity, carrier density and mobility in function of working pressure for ITO [7]

The figure shows that the mobility initially increases and stagnates around 0.8 Pa. This increase is more significant than the decrease in carrier concentration, which has already been clarified. The mobility depends strongly on the carrier scattering, which itself is related to defects (disclocations, precipitates and clusters). The generated argon ions are more likely to lose their energy by scattering in the higher pressure. However, the lower energy that remains can be better at forming the stochiometric structure. At a lower working pressure, the energy of the sputtered particles might be to high and allows electron scattering to have more influence on the growth of the film [7]. Taking both theories into consideration, it might be possible that both are

25

plausible but strongly depend on other parameters such as the flow rate, the geometry of the target/substrate or even the power. Another study [23] where ZnO films were deposited using magnetron sputtering reported similar results. A higher pressure caused a large increase of the resistivity because the lower bombardment created a less dense film and growth clusters that are further apart. However, this study also discusses some beneficial effects of a higher working pressure such as a smoother surface which made nucleation and growth easier.

It might also be possible that the effect of the working pressure is dependant on the particular deposition method that is employed. Furthermore, the enhanced reactive evaporation, which is causing the reduced resistivity, is limited to a very narrow range of the working pressure [8].

It is theorized in [6] that the oxygen vacancy defects decrease a films transmittance. Therefore, the transmittance increases with pressure because of the decrease of the free carrier concentration. This caused a decreased light absorption by plasmon resonance[3] in the ITO. An additional cause for a higher transmittance is that the film surface roughness decreases with increased pressure, which reduces the diffuse reflection. Figure 2.7 shows the transmittance in function of the different wavelengths, ranging from 300 to 800 nm, where each color represents the curve at a different working pressure. It is clear that starting from 4 to 15 mTorr, the transmittance increases from 77% to 91% at 500 nm.

This beneficial effect was verified by other studies, where it was observed that the high pressure promoted either an amorphous [7] or a column-shaped [7] crystallinity, which both interfere less with light, rather then a polycrystalline structure. The latter possesses a much higher density of grain boundaries, increasing the boundary scattering and reducing the transmittance.
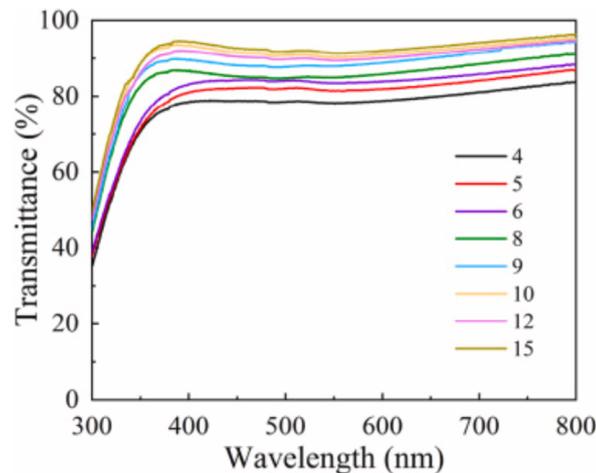
Figure 2.7: Transmittance at different working pressures [6]

It was observed in [6] and [7] that the deposition rate decreases. Figure 2.8 shows the resulting film thickness and the deposition rate in function of the working pressure. Both show a negative trend with an initial rise of the pressure, followed by a minimum and a slight recovery. This significant drop in the deposition rate might be explained by the decrease of the mean free path of the argon ions, which reduces the sputtering yield. Additionally, the sputtered target atoms (for ITO being indium, oxygen and tin) can scatter more easily, which impedes the incoming rate of sputtered atoms incident to the surface of the growing film. The decrease in thickness is crucial for understanding some of the experimental results in this thesis.

---

[3]Plasmon resonance is the collective oscillation of conduction electrons induced by an electromagnetic wave.
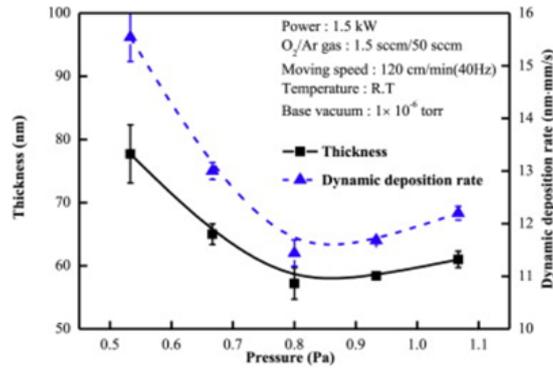
Figure 2.8: Thickness in function of working pressure for ITO [7]

2.5.3 Deposition time

Another parameter that could have an effect on the optoelectrical properties is the deposition time. It is the total time that the film is growing. The effect of this parameter has been discussed in [8]. As shown in figure 2.9, the resistivity has a minimum at 10 minutes of deposition. This figure also shows the influence of another sputtering parameter, being the target to substrate distance. The graphs show that the resistivity is lower at a smaller target to substrate distance, but that this effect is minimalized, again at 10 minutes. Changes to the target to substrate distance are unavailable for the sputtering tool used in Energyville.
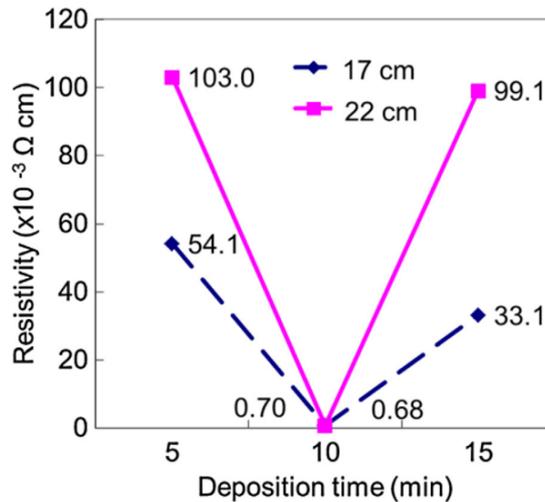
Figure 2.9: Resistivity in function of the deposition time for ITO [8]

The decrease in resistivity is attributed to an increase of the carrier mobility. This is caused by the low ionic impurity scattering in the amorphous ITO films [8]. It is theorized that the oxidation state depends on the deposition time, where 10 min yields the optimal oxidation conditions. A higher deposition time was observed to increase the temperature of the substrate, and thus an over-oxidation state occurs [26]. By contrast, a lower deposition time is insufficient to generate the temperature required to promote the growth of the film. For every specific tool, this optimum could be achieved at a different deposition time.

2.5.4 Sputtering power

The final sputtering parameter that will be discussed is the sputtering power. It is one the most dominant parameters of this deposition process and can have a major influence on not only the quality of the film, but also on process time and even thermal wear of the tool. Essentially, the energy flux increases when the power is ramped up. However, this relation is not necessarily linear, as is discussed in [18], chapter 7.3.1 and can deviate due to increased reflected neutrals, sputtering yield, gas heating effect, and the thermalization of energetic particles. It is important to realise that there are limits to which the power can be adjusted. For every target material and inert gas there is a minimum power, below which no sputtering will occur because the ions are not able to be formed, which can range from approximately 5 to 10%. On the other hand, the power can not be increased beyond a certain limit, because this could inadvertently degrade the sputtering target or cause mechanical stresses in the tool. There exists quite some research regarding the optimization of the sputtering power, such as in [13] and [9]. The latter reported on the effects that the sputtering power has on the resistivity and the transmittance of ITO films. Figure 2.10 shows the resistivity, carrier concentration and mobility in function of the sputtering power. The carrier concentration has an almost exponential increase when the power ranges from 50 to 150 W, while the mobility also has an initial increase but has a negative trend after 100 W. The overall result can be seen in a resistivity drop (from $4.4 to 2.9 \cdot 10^{-4} \Omega cm$).
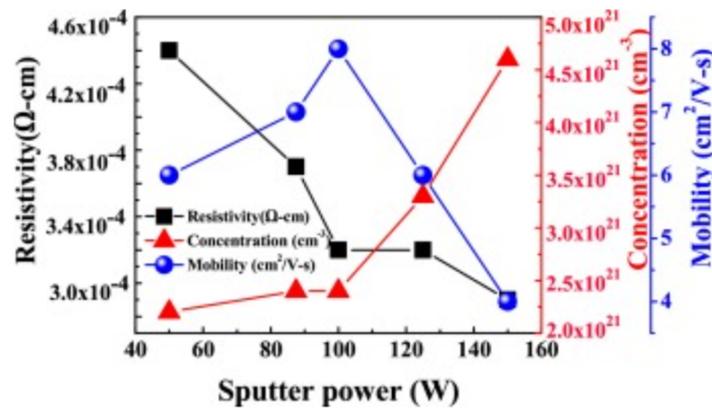
Figure 2.10: Resistivity in function of the sputtering power for ITO [9]

The decrease in resistivity can be because at low power, the grains grow with insufficient energy for crystallization to occur, resulting in an unstructured amorphous structure. The second publication [13] also reports a decrease in sheet resistance, this time for ITO deposited through RF sputtering on PET. It was speculated that the increase in RF power caused the bandgap to rise as well. This is attributed to the Burstein-Moss effect[4].

The first study [9] also analyzed the transmittance in function of the sputtering power. Figure 2.11 shows that the transmittance of the thin films in the NIR range decreased substantially as the sputtering power was increased to 150W. The transmittance curves in the visible light spectrum are shifted relative to each other because of interference at slightly different thicknesses. However, the mean transmittance for all ITO films is approximately 80%. The transmittance loss in the visible range can be explained with optical absorption and scattering, which is related to the impurity concentration, structural defects, surface roughness and grain boundary area.

---

[4]The Burstein-Moss effect occurs when the apparent band gap of a semiconductor is increased as the absorption edge is pushed to higher energies as a result of some states close to the conduction band being populated.
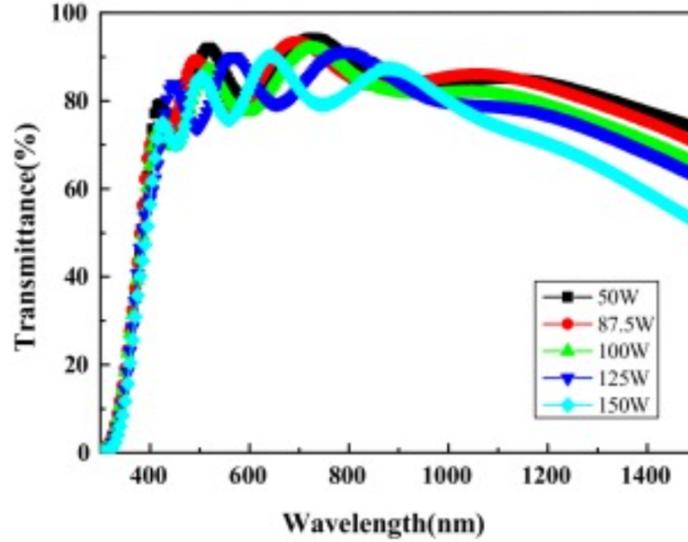
Figure 2.11: Transmittance in function of the sputtering power for ITO [9]

An important consideration is the sputtering damage, which is inevitably linked with the power changes. A thorough analysis of the induced damage can be found in [22], specifically for ZnO, which is a major focus of this thesis. The study found that the high energy plasma deteriorates not only the interface quality between the p-type absorber and the n-type ZnO, but also causes defects to form and grow on the absorber surface. A way to reduce this damage for DC-sputtering is to decrease the power. This also resulted in a higher resistivity, which is in fact beneficial to the ZnO layer since it functions as a short circuit barrier.

In conlusion, [22] reported that i-ZnO has two essential functions. The first one being a growth initiator for further ZnO:Al or ITO deposition, essentially enhancing the grain growth and possible reducing the sheet resistance. The second function is protecting the CIGS absorber fro sputtering damage and thereby increasing the fill factor.

2.5.5 Effects of thickness

In this section, the effect of the thickness, specifically of i-ZnO is discussed. The effect of the short circuit and protection barrier was studied [22] trough varying the intrinsic ZnO layer thickness. The study proposed that a thin (3 nm) intrinsic ZnO layer is higly beneficial to the performance of the CIGS cells. However, increasing the thickness of this i-ZnO layer too much, resulted in a worsening of the performance. Figure 2.12 shows how the thickness influences the performance of CIGS solar cells, expressed through the Fill Factor, Shunt resistance, Efficiency and Short circuit density.

As shown this figure, the shunt resistance of the cell was significantly improved, which results in a higher V_oc and conversion efficiency (from 10,1% to 11,8%). However, a further increase of the thickness to 170 nm decreased cell performance, severely limiting the J_sc due to the high resistivity (which is associated with the series resistance of the cells).

Essentially, the i-ZnO possesses a very high resistivity as concluded in [23] and in [10]. This improves the protection against short circuit defects. If this barrier is somehow thin in some regions, it can still hold back electrons from penetrating to the p-type absorber. The i-Zno layer

29

Figure 2.12: Effect of thickness of i-ZnO on CIGS cell performance [10]
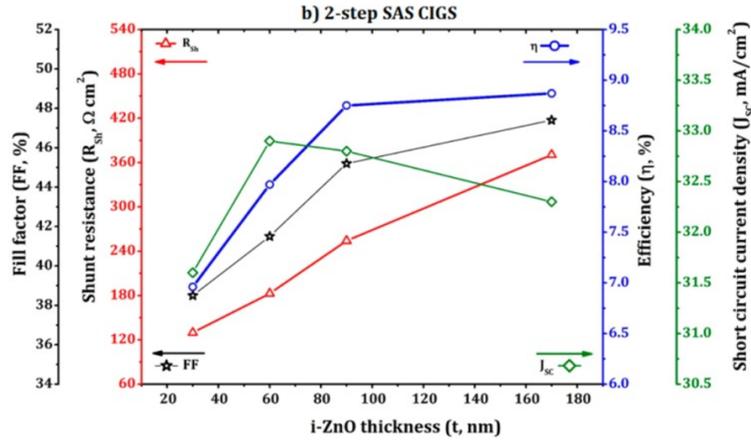
provides full coverage of possible shunt paths.

2.5.6   Effects of annealing

There exist many publications where annealing is used to drastically reduce the resistivity and increase the transmittance of TCO films. This seems to be a standard procedure when manufacturing screen coatings for many applications. One of these publications experimented with a range of annealing temperatures to understand the effect on resistivity and transmittance [27]. Both the carrier density and the optical band gap increased with higher annealing temperatures, stagnating around 250 °C. The increase in band gap and corresponding increase transmittance was again attributed to the Burstein-Moss shift as a result of a high concentration of free electrons, which can also explain the lower resistivity. The annealing in air improves the crystallinity of the films which results in a larger grain size. An additional effect is that the decreased density lowers the refractive index.

However, annealing is not mandatory if ITO is the final layer because of its many satisfactory properties. This enables ITO to deposited at the final state of the formation of multilayered structures for applications where an elevated temperature is not appropriate [4]

2.6   Conclusion

Firstly, PV terms were clarified and then the material class known as TCO was uncovered in light of current applications. Secondly, an introduction into deposition techniques and specifically sputtering process was provided. It can be concluded that RF sputtering provides a good film quality when depositing ZnO and ITO. The sputtering parameters that were discussed in this literature study are the gas mixture, the working pressure, the deposition time and the sputtering power. Additionally, the effect of annealing and ZnO thickness were analyzed. As a summary, these are the trends that were observed: an increase in oxygen improved transmittance and caused an initial drop of the resistance, but as the oxygen vacancies get filled, the resistance rises again. The working pressure has an unclear general effect on the resistivity. Some publications reported a decrease, others an increase. The effect is very dependable on other process conditions. The deposition time has to be controlled precisely to allow for a decrease in resistivity. Meanwhile, the power is beneficial for the conductivity, but detrimental to the transmittance. Also, the

power can not be too high to mitigate the damage to underlying layers. This damage can be prohibited by adding a protective i-ZnO barrier on top of the CdS. Finally, annealing the TCO significantly improves the optoelectric properties.

Chapter 3

Experimental methods

3.1 Sputtering tool

The performed depositions can be divided into two categories: sputtering on Soda Lime Glass (SLG) or sputtering on incomplete CIGS solar cells. ITO films were prepared on SLG for opto-electrical characterization by RF linear sputtering from a 66 by 12.7 cm ceramic target consisting of 90% In_2O_3 an 10% SnO. The sputtering tool is the Nebula Large Area Deposition tool from Angstöm Industries. It is capable of delivering 3000 Watts as sputtering sputtering power (This maximum power is achieved when the holder is completely filled with samples and the power parameter is set at 100%). The holder is able to fit substrates measuring 5 by 5 cm. To create solar cells, commercially available co-evaporated CIGS products were used as sputtering substrates. To prepare these samples, the window layers were first etched off with hydrochloric acid.

3.2 Characterization

To understand what the properties of the materials and solar cells are, sufficient information has to be gathered. They consist of thickness, electrical properties (sheet resistance, mobility, carrier concentration), optical properties (transmittance, reflectance and absorbance) and cell performance measures (IV-curves and efficiencies). Every subsection will focus on one of these measurements and describes how they have been performed. This includes the experimental setup and data types.

3.2.1 Thickness

The thickness of a TCO layer has a direct influence on the properties of that layer. For example, a thicker layer will cause a decrease in transmittance and sheet resistance. Therefore, it is a crucial geometrical property that needs to be measured for every sample. This provides perspective for the other properties and can explain some variations of the results. Only the properties of layers of similar thickness can be compared, provided that the thickness is not supposed to be a variable. The thickness was measured with the KLA-Tencor D-500 profilometer. To obtain consistent results, the parameters were as shown in table 3.1. Before the deposition, the middle of each sample was taped off to mask off a small strip. This allowed for a clean edge to be measured

with the profilometer, which was repeated six times to obtain the average and deviation.

Line length	1,2 mm
Needle speed	0,03 mm/s
Range	10 µm
Step mode	Step up
Stylus force	5 mg

Table 3.1: Profilometer parameters

3.2.2 Sheet resistance

The sheet resistance can be considered as a component of the series resistance in CIGS cells. It is determined with a number of probes by applying a voltage between two probes at a time and then measuring the generated current. The main setup used to measure the sheet resistance is a FPP5000 four point probe, which can give results with Ohm/sq as the unit. It is a very simple tool with which samples of almost any size can be measured. However, it cant measure sheet resistances higher then $4.5 \cdot 10^4 Ohm/sq$. For each sample, the measurement was repeated six times to obtain the average and deviation.

3.2.3 Mobility and carrier concentration

The mobility and carrier concentration are important parameters that can be used to derive the resistivity of a film. The carrier concentration (expressed in $/m^3$) is the number of charge carriers per unit of volume. The electrical mobility (expressed in $m^2/(Vs)$)is the ability of charged particles to move through a medium in response to an electric field. Both can be measured using a Hall-effect setup. It operates by measuring the generated current through four probes, first with just an applied voltage and in a later stage with a magnetic field of 1 Tesla that is applied with a permanent magnet. The setup also provides a resistivity which can be compared to results derived from the sheet resistance. To measure the samples, they have to be cut into squares of 1 by 1 cm, preferably with contacts (silver, indium or aluminum) soldered on the corners.

3.2.4 Transmittance, reflectance and absorbance

The transmittance, reflectance and absorbance of TCOs are essential properties to optimize. They determine how much light is able to pass through the window layers and which can be absorbed by the CIGS. All three of these properties can be expressed in a percentage, where 100% refers to all the light being transmitted, reflected or absorbed respectively. In theory, the sum of the transmittance, reflectance and absorbance should always be 100%. These optical characteristics were measured with a Bentham PVE 300 system. To enable that the output can be given in function of a series of discrete wavelengths, a TMC 300 monochromator was implemented. To measure the transmittance for every series of samples, first the signal counts of a silicon detector were measured, which serves as the 100% reference. Also a clean SLG sample was tested to observe what part of the spectrum is able to pass through just glass. For the reflectance, the silicon detector is also used as a signal reference. However, additional reference measurements were necessary to acquire a more realistic reflectance. These include the R0 measurement of the setup container and the R100 to take deviations (mostly at low wavelengths) into consideration. The absorbance was calculated during the data analysis, using Excel.

3.2.5   IV-curves and efficiency

The IV-curves provide the majority of information regarding solar cell performance. As shown in figure 2.1, the IV curve contains information about the short circuit current, the open circuit voltage, fill factor and allows for the conversion efficiency to be calculated using formula 2.2. This IV-characteristic is also called the illuminated curve. However, the solar cell can also be measured without any incandescent light, which is called the dark curve. The dark curve provides information about the diode behavior of the cell, like leakage current and forward bias voltage drop and current. The IV-characteristics were measured with a Keithley 2401 Sourcemeter, where an Oriel 91192-1000 provided the light source and corresponding air cooling of the lamp. To measure an array of solar cells, as shown in figure 3.1 , the sample was placed on a piece of glass if the substrate was flexible. Then the high probe was pushed down on the grid of a single cell, while the low probe was connected with the back contact of the array. The individual cells and back contact were created through a scribing procedure. To improve contact with the molybdenum back contact, usually elemental indium was applied through soldering. For the data analysis, a Matlab file processes the acquired curves to provide plots of the IV-curves and boxplots of the cell performance variables.
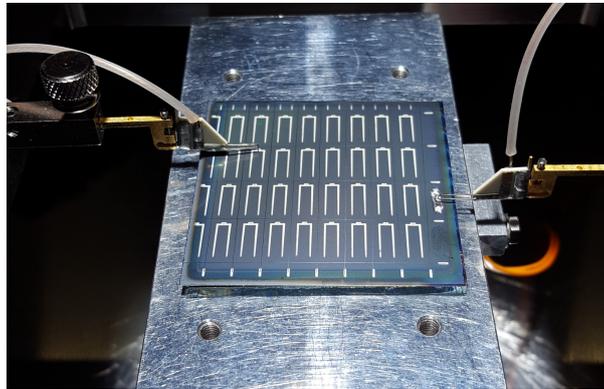
Figure 3.1: Method of measuring an array of solar cells (total of 32 complete cells) with the Oriel setup

3.3   Annealing

As mentioned in chapter two, annealing is a very effective way of increasing the transmittance and conductivity of a TCO. The working principle is nevertheless quite simple. For the annealing of samples, an ATD PEO 601 furnace was used. It allows for a wide range of conditions to be altered. These include the temperature, the annealing time, but also the addition of gasses such as nitrogen and oxygen. The gas flows can be programmed to occur anytime during the process and are able to be changed with manual gas flow controllers.

3.4   Previous measurements

The research into CIGS thin film PV at Energyville has seen much development. This resulted in a baseline recipe, which implements the best practice and most optimal process parameters for realising the currently best performing solar cells. The baseline has seen many changes throughout the years. However, a series of samples with the same recipe has been completed in

2019. This recipe consists of the best performing Mo, CIGS and CdS layers, with ZnO at 15 sccm Ar and ITO at 19.75 Ar and 0.25 sccm O_2 on top. For ZnO, the sputter tool was 25% for both ZnO and ITO. The window layers (ZnO and ITO) were deposited with varying thickness. Both the resistivity and transmittance were measured for these samples, the data of which was collected in a single Excel file. This data allows for the fluctuations of the complete sputtering process to be analyzed. It also provides much needed context for the results discussed in this thesis, because the previous results can be used to check if the improvements in resistivity and transmittance are significant or not. Figure 3.2 shows boxplots of the resistivity of the previous measurements for ZnO with ITO on top, but also for ITO and ZnO separately.
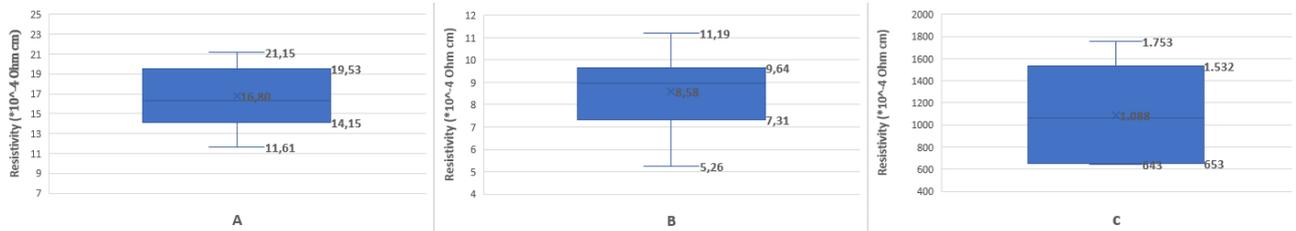

Figure 3.2: Resistivity of previous measurements. A) ZnO + ITO, 17 samples B) Only ITO, 24 samples C) Only ZnO, 7 samples

For these boxplots, a resistance difference larger then the interquartile range, which contains 50% of all the could be perceived as significant. For ITO, this means that a resistivity drop larger then $2.3 \cdot 10^{-4} \Omega cm$ could indicate that the recipe change has a significant effect. For ZnO, this minimal difference has to be $879 \cdot 10^{-4} \Omega cm$. The effect of the fluctuations can also be analyzed for the transmittance curves of samples with the same recipe. Figure 3.3 shows the transmittance, gathered by previous measurements, for ZnO with ITO on top, but again also for ITO and ZnO.
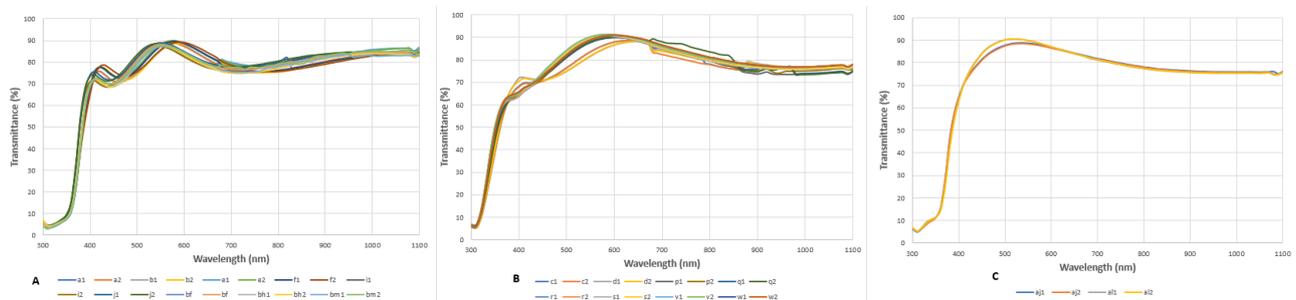
Figure 3.3: Transmittance of previous measurements. A) ZnO (120 nm) + ITO (150 nm), 18 samples B) Only ITO (150 nm), 16 samples C) Only ZnO (120 nm), 4 samples

Here, the absolute difference between the top and bottom transmittance curves could be considered to be the total possible deviation. For ZnO + ITO, this is circa 4.4% (83.2% - 78.8%) at 900 nm. This amount of spread seems to be consistent across the light spectrum. For ITO, this deviation varies from 2,1% at 500 nm (without outliers) to 2,9%. For ZnO, this deviation is 2,6% at 500 nm.

The fluctuations can be attributed to many factors. The main distinction is that some factors are determined by the procedure of the sputtering itself, others by the sputtering process and then also some by the measurement errors. These includes, but are not limited to: the choice of the holder, the placement of the samples in the holder and waiting time in between depositions. The other factors can be attributed to the actual deposition itself. These include: preceding

sputtering sequences (for example, depositing ITO right after ZnO might cause an increase in resistivity), variations in the gas composition and fluctuations in the power level. Additionally, the roughness, grain size and general quality of preceding layers in the PV stack can massively influence the properties of the window layers. Finally, the measurement error on the data acquired by the spectral analyzer, the four point probe and the profilometer have to be considered. At the very least, these can cause up to 5% variations in the results.

3.5   Procedure analysis

This final section about the procedure analysis is closely linked to the experimental methods. During the experiments that were conducted to optimize the sputtering parameters, sometimes inexplicable property changes occurred. For example, when analysing the effect of changes to the working pressure during the sputtering of ITO, a similar recipe was used to create several samples, to test the repeatability of the sputtering tool. There was a significant variation in both sheet resistance and transmittance between two samples. The sheet resistance seemed to increase from 41 Ω/sq to 50 Ω/sq, while maintaining the same thickness, working pressure and other process conditions. The only difference was that different holders were used in the sputtering tool. Apparently, using two different holders one after another to speed up the experiment, causes a worsening of the optoelectrical properties of the ITO. This is faster since the loading chamber does not have to vented to take out the samples and put new substrates in the holder. To single out this factor, three samples were created: one with the normal procedure of ITO sputtering, one with the same holder but directly after the first run and one where a different holder was used directly after the first deposition on the first holder was done. The recipe is the same as the baseline described in 3.4. The sheet resistances of these three samples are listed in table 3.2.

Name of procedure	Sheet resistance (Ohm/sq)
Normal procedure	0.42
Same holder	0.45
Holder 2 directly after	0.79

Table 3.2: Procedure analysis sputtering

As can be seen in the table above, the sheet resistance increases significantly when the wrong holder is used. There is also an impact on the transmittance, as can be seen in figure 3.4.
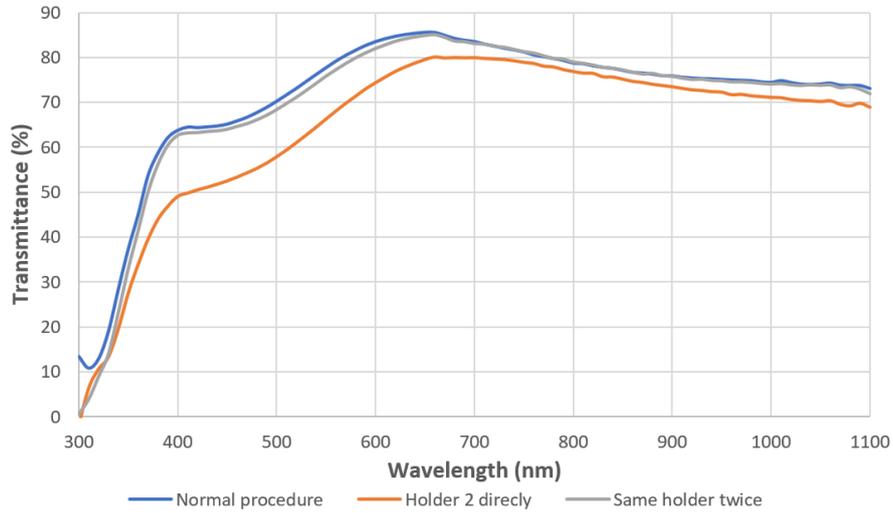
Figure 3.4: Transmittance of ITO with same recipe but different procedure

The transmittance of the normal procedure is very similar to the transmittance when the same holder is used twice. The small variations can be explained due to fluctuations as discussed before. However, when using holder #2 after holder #1, the sample seems to visibly opaque, as is verified in the figure above. There is a significant drop of transmittance around the visible wavelengths. This reduction in the optical quality will be taken in to consideration in later discussions. Especially when solar cell performance will be analyzed, this drop in transmittance will allow less light to pass through to the CIGS absorption layer and thereby decrease the short circuit current. In conclusion, the procedure analysis is an important factor to interpreting the gathered data.

Chapter 4

Results and discussion

4.1 Working pressure changes

In the first series of experiments, the influence of the working pressure was be investigated. As explained in 2.5.2, changing the working pressure will primarily change the concentrations of Argon ions during the sputtering. This will affect the sputtering mechanism, as the target particles now interact with more obstacles in their mean path towards the substrate. For the baseline sputtering process, the standard working pressure is 3 mTorr[1]. To include all the possible effects, ITO and ZnO samples were sputtered at 2, 3, 4 and 9 mTorr. A full characterization of the film requires a measurement of the thickness, resistivity, optical properties (which are the transmittance, the reflectance and the absorbance). Additionally, the solar cell performance and stability will be investigated.

4.1.1 Deposition rate

By measuring the thickness of each sample, the deposition rate can be estimated. This has several consequences for other characteristics. The thickness was measured six times for each samples. Figure 4.1 plots the thickness of ITO and ZnO samples at different working pressures.
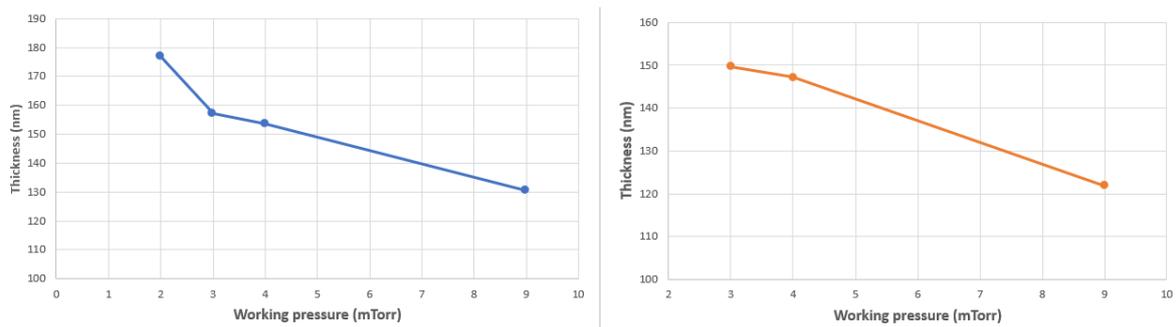

Figure 4.1: Thickness in function of working pressure for ITO (left) and ZnO (right)

It is clear that for both materials, the thickness is lower at a higher pressure. When changing the pressure form 3 to 9 mTorr, the thickness decreases from 160 nm to 130 nm. This is similar to

---

[1]For reference, 3 mTorr is equal to 0.4 Pa.

findings in other studies where the working pressure was investigated. The reason for this change was discussed in 2.5.5, where it was theorized that a larger number of Argon obstacles directly reduces the sputtering yield. The mean energy of the generated Argon ions is lowered, resulting in less ions with a kinetic energy higher then the threshold, at which target particles would be sputtered off. These lower energy ions essentially bounce off the ITO/ZnO film. Therefore, the deposition rate is inversely proportional to the working pressure.

4.1.2   Resistivity

The resistivity was measured with the four point probe and the hall measurement setup. The two methods can thereby verify each others results. The four point prove provides the sheet resistance and can therefore only be used for comparison when multiplied by the thickness. For the initial experiment with varying pressure, each deposition consisted of two samples. One was placed in the middle of the holder, while the other one was placed in the corner of the holder. This was done to examine the effect that the position of the sample has on the deposition quality. Figure 4.2 shows the variation of the resistivity in function of the working pressure for the analyzed ITO samples. The blue markers indicate the samples put in the corner of the holder, while the orange markers indicate the middle samples. The left plot is the data gathered with the four point probe, while the right plot is the data obtained with the Hall setup.
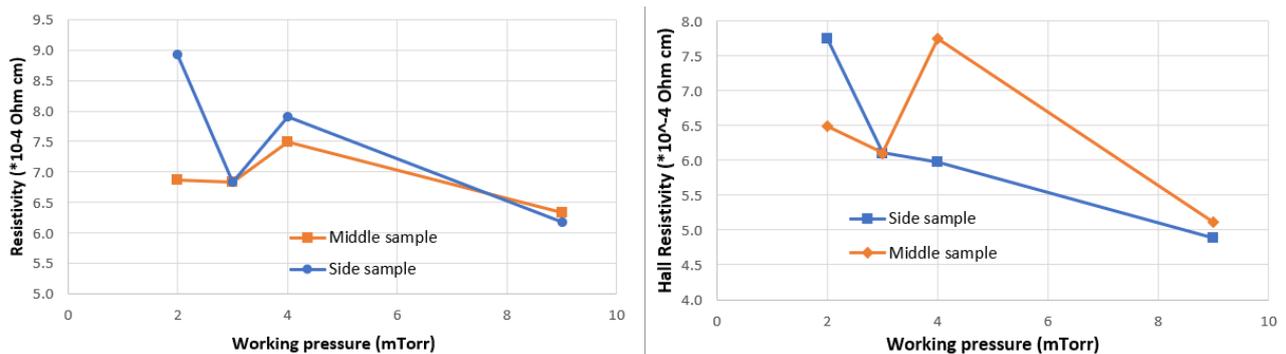

Figure 4.2: Resistivity in function of working pressure of ITO film. Left plot is with four point probe and right plot with Hall setup

By looking at the plots, its not instantly obvious what the trend seems to be. The sudden surge in resistivity from 3 to 4 mTorr is present because the reference sample at 3 mTorr was created a few weeks earlier, while the other samples were deposited in one succession. Therefore, it can simply be caused by fluctuations, which were clarified in the previous chapter. Furthermore, the difference between the middle and side sample is consistent. Also, the curve for the middle samples obtained with the Hall setup is generally higher than the one for the side samples. In contrast, the difference between middle and side resistance is lower for the four point probe. Also, the four point probe resistivity measurement seems to be slightly higher then that for the Hall setup. In general, there seems to be a downward trend of the resistivity as the working pressure increases. For the side samples, the resistance gathered with the four point probe decreases from 7.8 to $6.2 \cdot 10^{-4} \Omega cm$, which is a difference of $1.6 \cdot 10^{-4} \Omega cm$. As discussed in section 3.4, the minimum resistivity difference for ITO is $2.3 \cdot 10^{-4} \Omega cm$. Therefore, it can be said that the effect of the imposed increase of pressure on the resistivity of ITO is insignificant. This does not conclude that increasing the pressure has no effect on resistivity. It could be hypothesised that the drop in resistivity could only occur with even higher pressures, as discussed in 2.5.2. In

theory this is possible with the sputtering tool in Energyville. However, in consultation with the research group, it was decided not to experiment with higher pressure, because it was observed that a working pressure of 9 mTorr already resulted in an enlarged plasma volume. So to not damage the tool, 9 mTorr could be considered a safe limit.

To verify these results and to figure out the internal mechanisms that cause this, albeit not so significant, decrease in resistivity, the mobility and the carrier concentration were also measured. The conductivity of a material is directly proportional to these two properties. Figure 4.3 plots the mobility and the carrier concentration of the same samples as analyzed before, also in function of the working pressure.
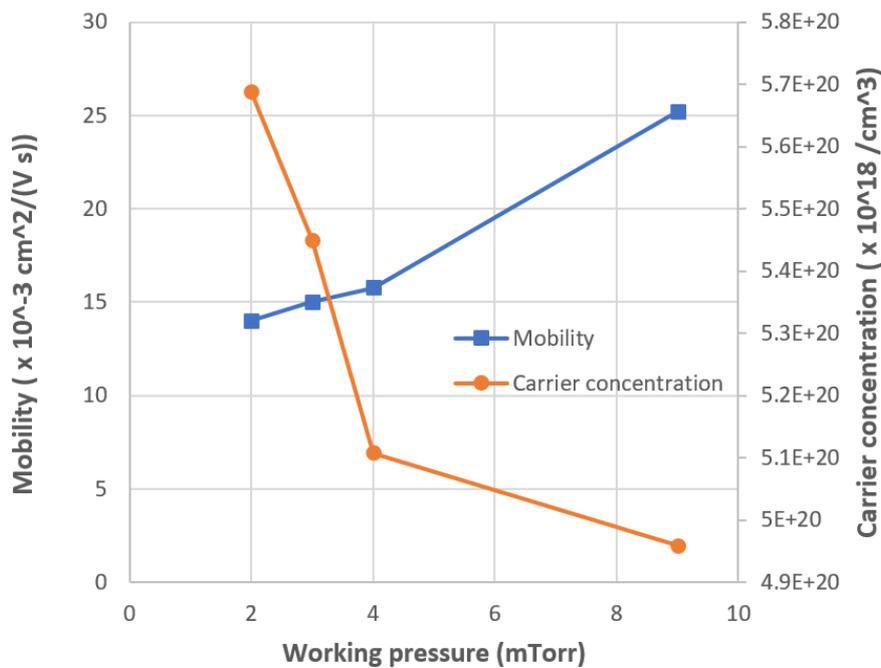

Figure 4.3: Mobility and carrier concentration in function of the working pressure for ITO

The mobility increases with the pressure, from 14 to 25 $\cdot 10^{-3} cm^2/(V \cdot s)$. This can be explained because of the softer sputtering which results in less defects, which act as obstacles. The mobility is therefore the main influence for the downward resistivity trend. However, this influence is opposed by the significant drop of the carrier concentration, as is also shown in 4.3. This initial drop and following stagnation are related to the partial pressure of oxygen that also rises, which causes the oxygen vacancies to be filled. The oxygen vacancies had introduced two electrons in the film, and therefore the conductivity is reduced [21]. This counteracts the effect that the increase in mobility has, but not completely, since there is still a slight trend visible in 4.2. These particular trends of the mobility and the carrier concentration with varying pressure were also observed in [7].

The same experiment was also conducted for ZnO film. This metal-oxide is much more resistive than ITO since zinc is less conductive then indium and tin. This is what makes it a desirable material to be used as a short circuit carrier. However, because of the high resistivity, measuring the ZnO films could not be performed with the four point probe nor the Hall setup. Therefore, a different measuring method was introduced. With the probes of the Keithley 2401 Sourcemeter, it is possible to measure the current in function of an applied voltage. Figure 4.4 indicates that with a correct measurement, the IV-curve is linear. With Excel, a trendline was obtained, of

which the slope is an indicator of the resistance. It is clear that the fit is not perfect (R^2 is 0.9978), which means that there is a large error on this result. The unit of this result is Ohm and therefore the ZnO results can not easily be compared to the resistivity of ITO.
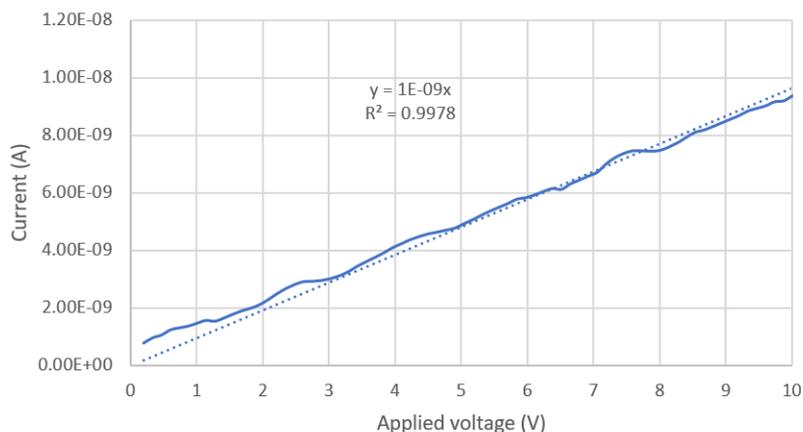

Figure 4.4: Linear relation of current and applied voltage to measure the resistivity of ZnO

With this IV method, the resistances of several ZnO films at different working pressures were obtained. Figure 4.5 shows a plot of these results for both side and middle samples, starting at 3 mTorr.
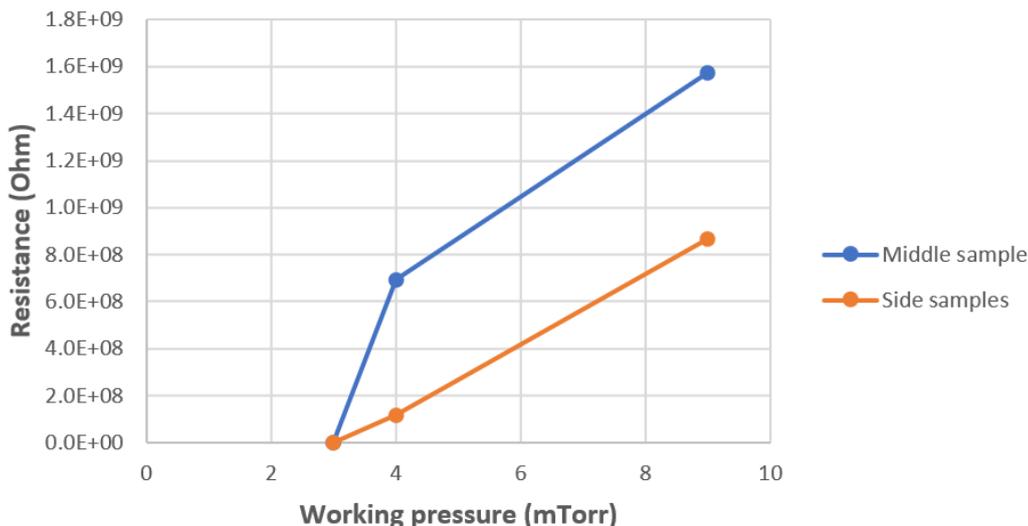
Figure 4.5: Resistance in function of working pressure for ZnO

At first glance, it is clear that the resistance surges several orders of magnitude when depositing in higher working pressure. Overall, the resistance of the side samples does seems to be lower then for the middle samples. For the middle sample, the resistance rises from $0.38 K\Omega$ to $1.57 M\Omega$, which is $4.1 \cdot 10^3$ times higher. This high resistivity could be very beneficial to the protecting ZnO layer when deposited on the previous layers of the CIGS solar stack.

The increase in resistance can be explained through the deposition mechanism at higher sputtering. The high velocity of the atoms at lower pressures leads to more defects in the film structure. These defects could be linked to oxygen vacancies, resulting in a more conductive ZnO film. This is in agreement with the conclusion of 2.5.1. Even though the range of pressure is relatively

small, a large resistance variation was obtained. This explanation is also given by [28], where an even higher rise in resistivity was observed (from $10^1 \Omega cm$ to $10^8 \Omega cm$), when ranging the working pressure from 3 to 10 mTorr.

4.1.3 Optical properties

The optimization of the transmittance is an equally important aspect of this thesis. The ITO and ZnO samples used to determine the resistivity can be used to measure the transmittance, reflectance and absorbance. To put the spectral results into perspective, first the transmittance was measured without any substrate and secondly with a clean SLG-substrate. The first reference indicates what the measurement error is in function of the wavelength. The second reference provides information about which wavelengths are not able to pass through the SLG and also about the maximum limit to the transparency. These two references, together with the transmittance curves at different working pressures is plotted in figure 4.6.
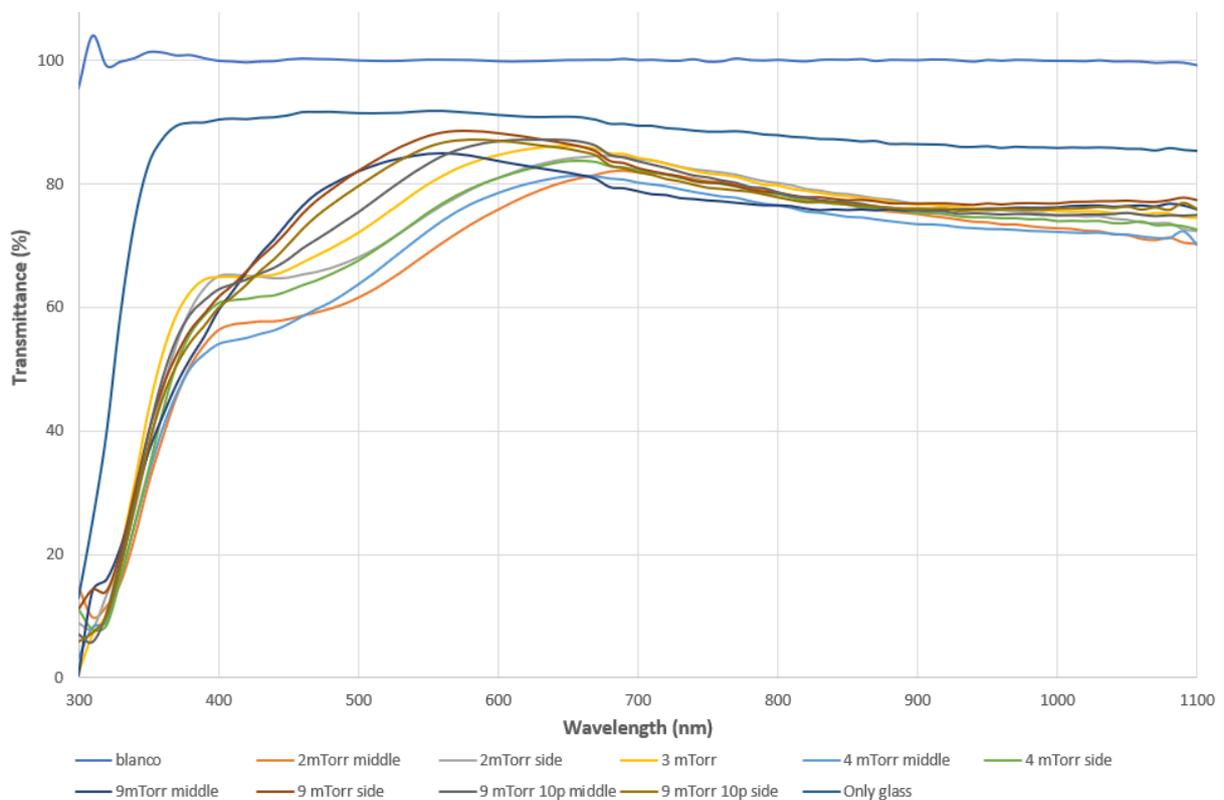
Figure 4.6: Transmittance of ITO in function of wavelength at different working pressures

The first reference shows that at short wavelengths, the error is relatively high. At higher wavelengths, this error seems to fluctuate about 1% around 100%. Furthermore, transmittance curve for only glass indicates that any wavelength lower then +/- 350 nm gets blocked by the glass itself. This UV-cut off is common for soda lime glass. The peak transmittance is 92% at 560 nm. At higher wavelengths, the transmittance declines slowly, until it reaches 85% at 1100 nm. The transmittance curves of ITO on glass show a similar pattern, but with a UV-cut off around 400 nm. The maximum seems to be higher and shift to lower wavelengths as the working pressure increases. This trend however, is not because the optical quality increases, but because the thickness of the ITO film is significantly lower, absorbing less light. This is also shown on figure 4.7, where only the transmittance curves of the middle samples are plotted, in

addition to the corresponding absorbance. Because of this, there is not actual improvement of the transmittance.
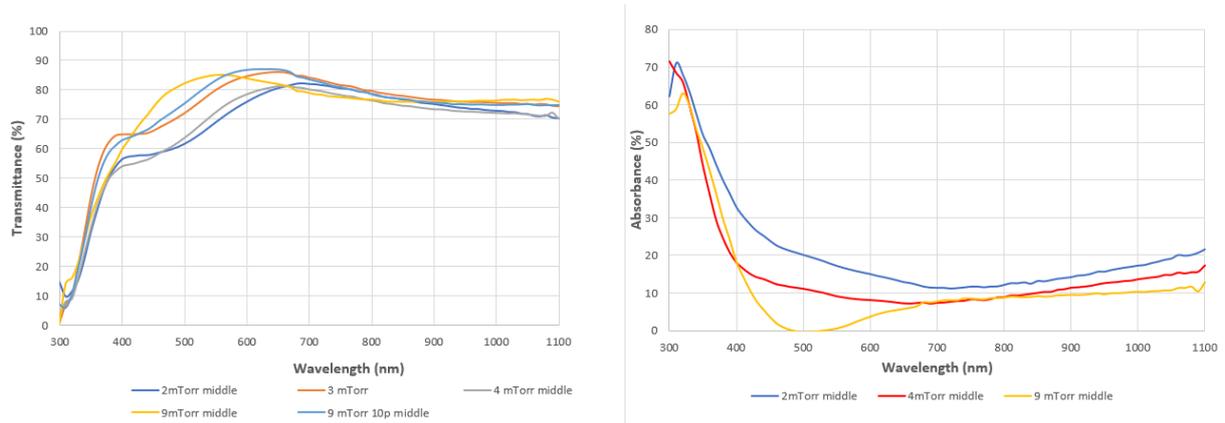
Figure 4.7: Transmittance and absorbance of ITO in function of wavelength at different working pressures

4.1.4 Solar cell performance

The solar cell performance is arguably the most important analysis. The optimization of the optoelectrical properties only serve to improve a solar cells ability to conduct the generated electrons and let through as much light as possible. Therefore, the insignificant decrease of the resistivity will presumably not result in a performance increase. However, the sputtering at a higher working pressure might be beneficial in other ways. For this reason, figure 4.8 provides an overview of the essential performance characteristics (including the conversion efficiency, the fill factor, the short circuit current and the open circuit voltage). In addition to the characteristics, measured right after completion of the cells, for both 3 and 9 mTorr, two more data sets were obtained. The samples were measured again twice, once after two weeks and once after a month, to investigate the stability of the solar cells. This is indicated with numbers: 1) directly after deposition, 2) after two weeks, 3) after one month.

Figure 4.8: Solar performance characteristics at 3 mTorr (baseline) and 9 mTorr. Top left: Efficiency. Top right: Fill Factor. Bottom left: short circuit current. Bottom right: open circuit voltage
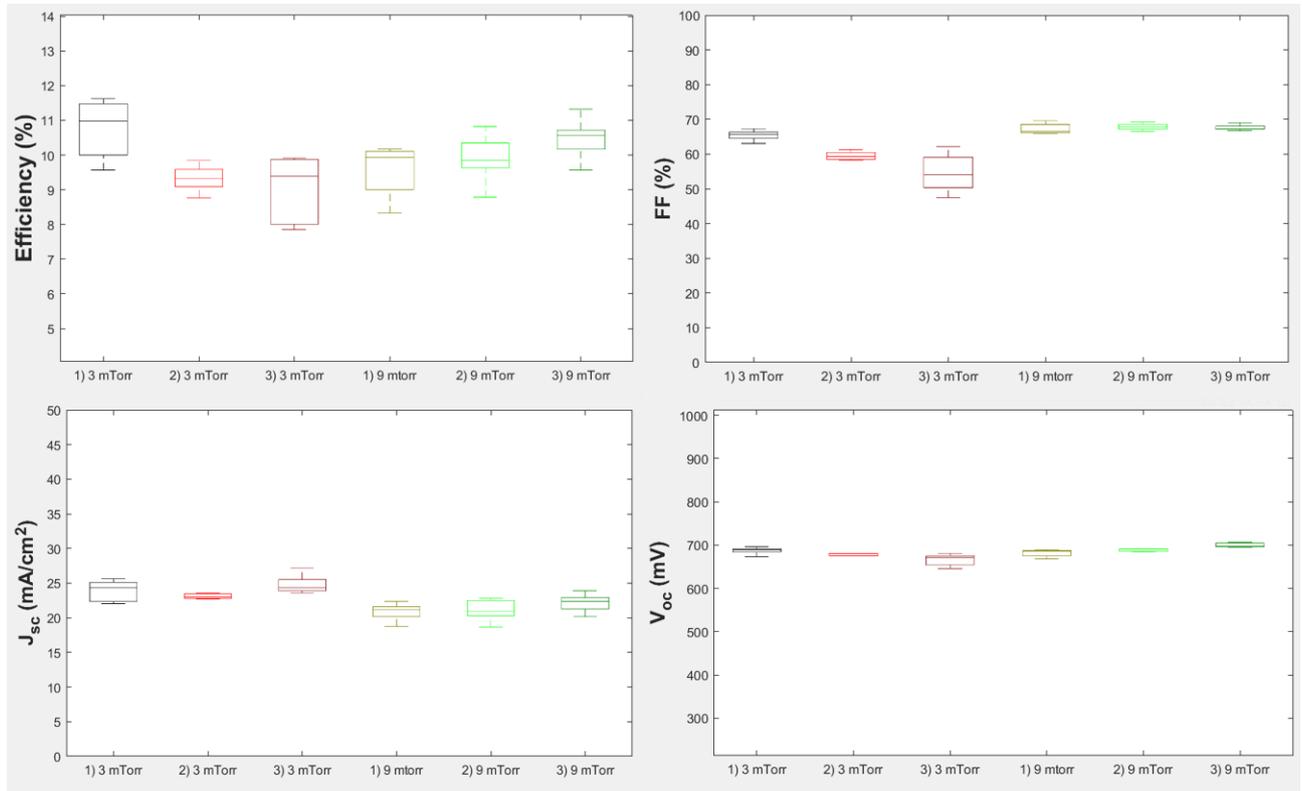
The efficiency seems to decrease with a higher pressure. However, it was later detected that the sample at 9 mTorr contained ZnO and ITO, sputtered with the wrong procedure, as discussed in 3.5. This caused a significant increase in resistivity and transmittance. The transmittance is essentially a measure to express how much light is able to pass through the window layers. Therefore, the short circuit current should be directly proportional to the transmittance. To take this into consideration, it is possible to compensate for the loss of light by increasing the conversion efficiency. This amount can be considered to be the same as the loss of short circuit current. For the 9 mTorr sample, this would result in an increase of the median efficiency of 1.4%, since the J_{sc} increases by 14%. To verify this amount, the mean value of the transmittance curves in figure 3.4, as discussed in section 3.5, can be compared. The mean transmittance of the normal procedure is 67%, while that of the procedure where holder 2 is used is 63%. This is relative decrease of 19%, which results in 1.9% for the conversion efficiency. The resulting values are relatively similar.

Now all the performance characteristics can be interpreted. Following the previous calculations, the efficiency of both 3 and 9 mTorr are almost the same (11.7% and 11.4%). However, the Fill Factor is significantly higher at 9 mTorr, which indicates that there might be less defects. This is in line with the conclusions discussed in section 2.5.2, where it was theorized that the higher working pressures reduced the kinetic energy of the sputtered target atoms. This softer sputtering may explain the reduced damage. The open circuit voltage however seems to be quite similar at both pressures.

The most promising result however is found not in the characteristics, but in the stability of this

performance. The sample created at 3 mTorr seems to degrade considerably after two weeks, with the median efficiency dropping from 11 to 9.5%. After one month, the median efficiency did not decrease, but some specific cells did lose performance, with efficiencies dropping to 8.7%. This efficiency loss can be attributed to the almost linear decrease of the fill factor. This degradation is in stark contrast to that of the 9 mTorr samples. The degradation of these solar cells is not noticeable in the efficiencies nor the fill factor. The performance seems to increase over time, mainly due to an increase of the open circuit voltage. This could be attributed to the light-soaking effect, as discussed in [29]. This study investigated the effect of light-soaking on the solar performances. Here, a constant illumination lasting 60 min seemed to improve the V_{oc} and the FF, and therefore also the conversion efficiency. The major reason for this was claimed to be in particular the soaking of UV light, which forms a p+ defect layer in the CIGS absorber near the interface and its subsequent neutralization by electrons generated selectively by UV light in the buffer layer. The reported increase in V_{oc} and FF is quite similar to the one observed in 4.8. In any case, it is clear that the short-term degradation is seemingly reversed for cells sputtered at 9 mTorr.

Degradation occurs through two main principles, being oxidation and room temperature diffusion.The first cause presumably has less impact, since the window layers are not prone to oxidation. In contrast, the room temperature diffusion causes unstable regions to transform into defects. This is because the samples are being stored in a climate controlled space (at around 20°C). The mitigated degradation could be explained through a reduced amount of defects. It is possible that a higher pressure creates less disturbances in the atomic structure and therefore reduces the concentration of unstable regions, which would otherwise evolve into defects.

A second and complementary explanation could be that the higher pressure, besides introducing more argon atoms, also influences the partial oxygen pressure. This excess of oxygen atoms could fill the already existing oxygen deficiencies, as discussed in [21]. They claim that the increase of oxygen reduces structural lattice defects.

4.2   Carrier speed changes

Another parameter that could still be optimized is the movement speed of the carrier which contains the holder. In turn, this holder contains the substrates. The speed can range from a maximum of 20 mm/s to 1 mm/s. The carrier speed directly determines how much atoms are deposited in one pass of the sputtering process. The longer exposure time of the deposition has to be compensated by reducing the number of passes to maintain the thickness of the film. There might be an effect on the density and the crystal structure of the TCO. A possible hypothesis is that reducing the number of passes creates less interfaces, which can occur when a new layer of atoms does not integrate well with the film that is already present. As a result, the transmittance would be lower and the homogeneity could be improved, increasing the mobility and thus the conductivity. This hypothetical effect of the carrier speed reduction is shown in figure 4.9. An additional effect could be that the temperature would rise during the deposition, which could improve the crystal quality.
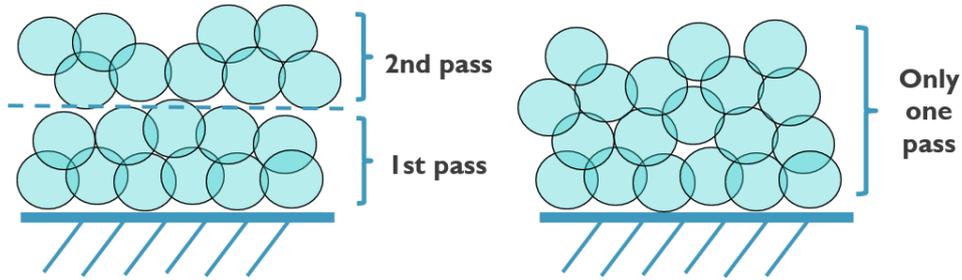
Figure 4.9: Hypothetical effect of carrier speed reduction

4.2.1 Resistivity

The method of obtaining the resistivity values for carrier speed variations is similar to that of the pressure experiment as discussed before. An initial test was performed to observe the general trend. this test consisted of one batch deposited at 9 mm/s for 4 passes and a second batch at 4.5 mm/s for 2 passes. Compared to baseline ITO, these films are thinner and are therefore more resistive. Figure 4.10 shows the resistivity for the middle and side sample at both carrier speeds.
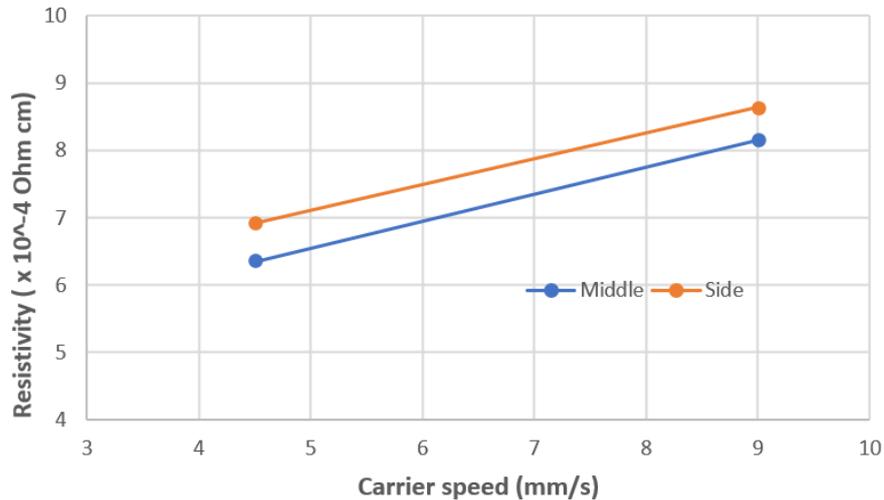

Figure 4.10: Resistivity in function of carrier speed of a thicker layer of ITO

It seems that at a lower carrier speed, the resistivity decreases by $1.7 \cdot 10^{-4} Ohmcm$ for the middle sample. As discussed in the section about the previous measurements, a change of the resistivity of ITO is only significant if it is greater then $2.3 \cdot 10^{-4} Ohmcm$. Therefore, the observed reduction is not very meaningful. To reproduce this downward trend and see if at even lower speeds, the decrease is more noticeable, different ITO samples were created with the speed varying from 20 to 1 mm/s. Figure 4.11 shows a plot of the resistivity obtained by a second set of experiments. For the baseline recipe, 9 mm/s is used. To investigate a more broad range, lower and higher speeds were tested. To compensate for the deposition rate, the amount of passes range from 1 at 1 mm/s to 20 at 20 mm/s, which deposits a film of around 150 nm thick.

A similar downward trend, which is almost linear, can be observed. However, the resistivity only varies from 7.5 to $6.3 \cdot 10^{-4} Ohmcm$, which is not significant. Taking both series of experiments into consideration, it can be said that there seems to be a negative trend in the resistivity but that changing the carrier speed does not make a relevant change to the resistivity.
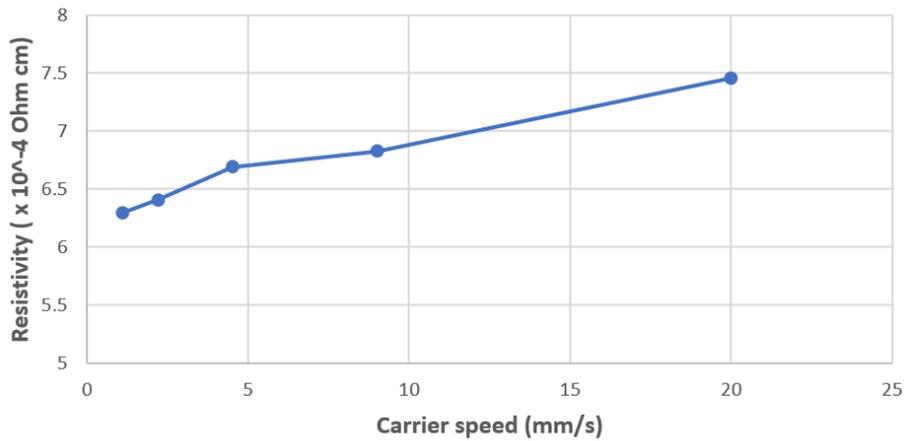
Figure 4.11: Resistivity in function of carrier speed of a thicker layer of ITO

4.2.2 Optical properties

In addition to the resistivity also the transmittance, reflectance and absorbance were measured. Figure 4.12 plots the transmittance curves for samples created at a speed which varies from 2.2 to 10 mm/s.
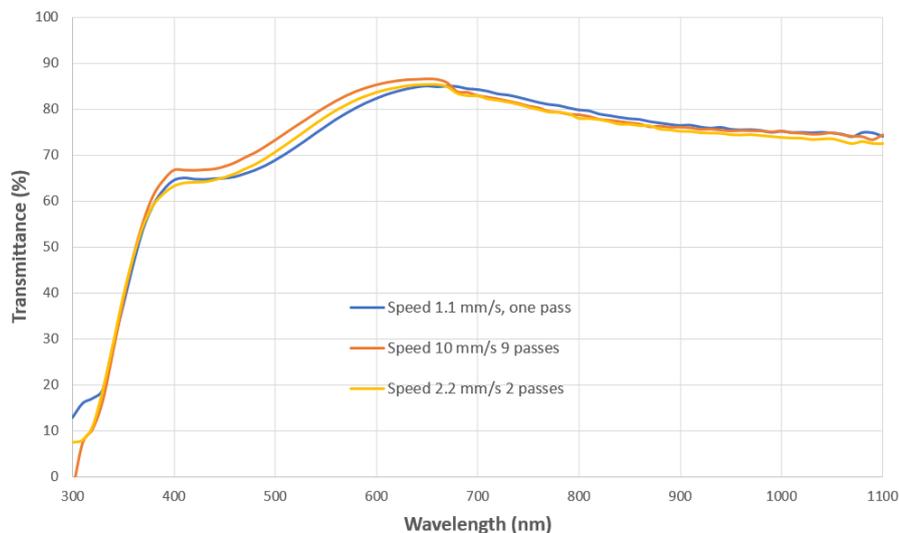
Figure 4.12: Transmittance in function of wavelength at different carrier speeds for ITO with a thickness of 150 nm

The transmittance curves only vary slightly relative to each other. The variations reach a maximum of 6% at 540 nm, due to the shifting of the peaks. The variation elsewhere is only a few percent, which can be attributed to fluctuations of the sputtering process. In addition, figure 4.13 shows the reflectance and absorbance for all created samples (including middle and side samples).

It appears that for both reflectance and absorbance, the influence of the carrier speed is minimal. All variations can be attributed to fluctuations. In conclusion, the carrier speed does not seem to have an effect on the optical properties of ITO. The effect of this parameter was not investigated for ZnO since the experiments with ITO yielded no significant improvements.
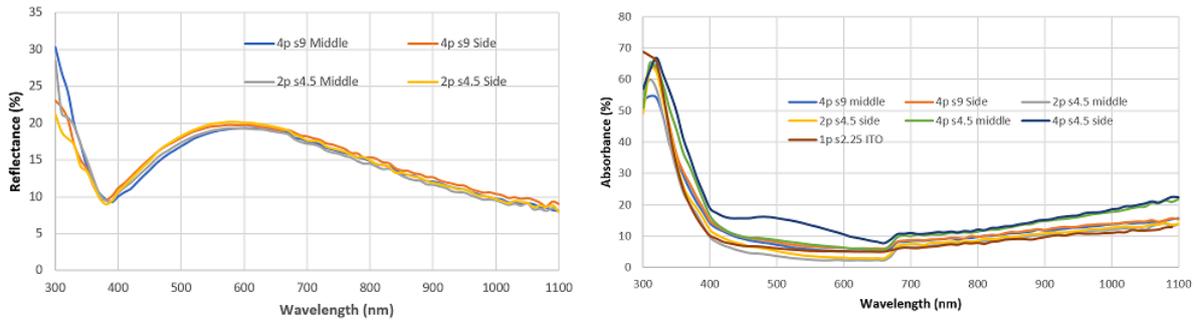
Figure 4.13: Reflectance and absorbance in function of wavelength at different carrier speeds for ITO with a thickness of 150 nm

4.2.3 Solar cell performance

As mentioned in the hypothesis, the carrier speed might have an influence on the deposition mechanism. The crystal growth might be more refined, comparable to an annealing effect. A similar overview of the results for the effects that the working pressure has on the solar cell performance can be provided. The performance characteristics are given in figure 4.14. It is important to note that the deposition of the ITO for the last sample, where a speed of 2.2 mm/s was used, got stopped prematurely. Because the deposition time was increased considerably, the sputtering tool timed out after only one pass. This timeout parameter was later disabled.

Figure 4.14: Performance characteristics for the reference sample and at 9 passes (speed is 9 mm/s), 4 passes (speed is 4 mm/s) and 1 pass (speed is 2.2 mm/s). Top left: Efficiency. Top right: Fill Factor. Bottom left: short circuit current. Bottom right: open circuit voltage

At a first glance it is clear that the efficiency decreases with less passes in combination with a lower speed. This dec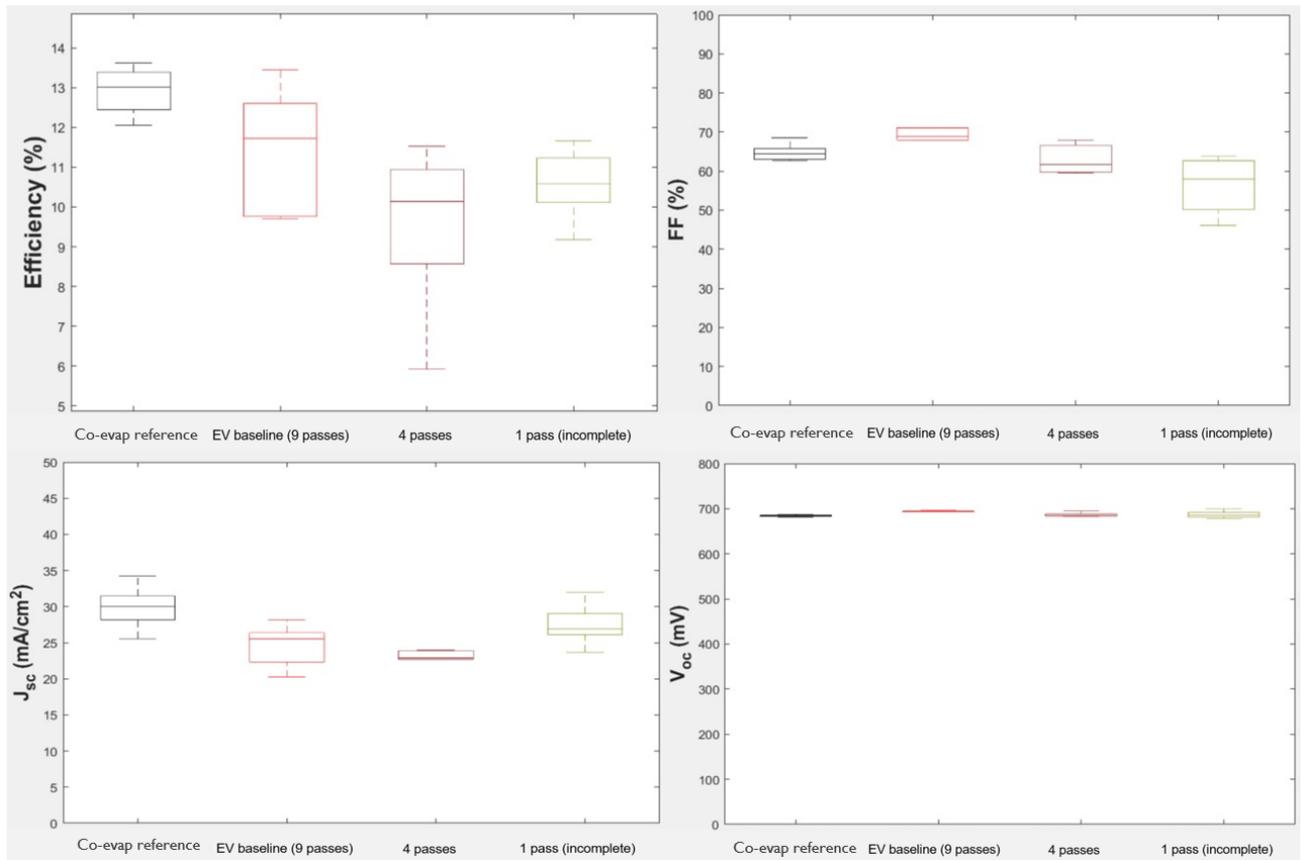rease is caused by the worsening of the fill factor and the short circuit current. The fill factor problem is mainly attributed to defects in the absorber layer. The main cause for this is unclear, but a possible explanation might be that a prolonged exposure to incoming sputtered particles might roughen up the already deposited film and induce damage to the underlying layers. The slower the carrier speed, the longer every section is exposed to impacting particles. Furthermore, there is no significant change to the open circuit voltage. The short circuit current decreases, which is not due to a lower transmittance but because of a high series resistance. This characteristic is however higher for the uncompleted sample, since the ITO is only half as thick and lets through more light.

4.3   Power changes

The level of power determines many aspects of the sputtering process. It is directly proportional to the sputtering yield, which is the ratio of the sputtered target atoms to the incident ions. A lower power introduces less energy, which is controlled through the applied voltage. Lowering the voltage means that the generated electromagnetic field is less strong and in turn causes the generated ions to not accelerate as much, providing them with less kinetic energy. However, there is a minimum power, below which the gas wont transform into plasma (which is called the ignition of the plasma).

During the analysis of the ZnO deposition step, it was recognized that the power was not yet altered in preceding internal research. Specifically lowering the power for the first few ZnO passes might induce less damage to the underlying layers. These first few passes are deposited without an oxygen inflow. After the oxygen deficient ZnO, another 7 passes of ZnO with 0.1 sccm oxygen were deposited. Table 4.1 shows the different power changes that were tested, together with their corresponding amount of passes. As can be seen, a lower power necessitates more passes because the sputtering yield is lower.

Experiment	1	2	3
Recipe	10% 1 pass	10% 2 passes	6% 6 passes
Thickness (nm)	37	60	51

Table 4.1: ZnO power changes experiments

Before analysing the solar cell performance, it is necessary to look for any influence that changing the sputtering power might have on the resistance and the transmittance of the ZnO layer.

4.3.1   Resistivity

Because the small thickness of i-ZnO inside the CIGS cells, the sheet resistance of the ZnO layers is too high to be measured using the four-point probe. As discussed in 4.1.2., ZnO resistances can be compared to each other by the slope of the IV-curves. These curves were also measured for the new power recipes as summarized in 4.1. The results of the resistances, together with the thickness are given in table 4.2. This table also provides a multiplication of the resistance and thickness, resulting in a measurement which relates to resistivity. It is important to add that this measurement is not identical to the resistivity as obtained in previous paragraphs. The presented thickness also includes the additional 7 passes where oxygen is added.

Recipe	25% 20 passes	10% 1 pass	10% 2 passes	6% 6 passes
Resistance ($\cdot 10^5$ Ohm)	3.83	55.4	21.4	38.3
Thickness (nm)	150	37	60	51
Resistivity (Ohm cm)	5.74	2.05	1.28	1.96

Table 4.2: Effects of power changes on resistivity of ZnO

The resistivity results show that by decreasing the sputtering power from 25 to 10 %, the resistivity is halved. This effect was explained in 2.5.4, where it was explained that the lower power causes the grains to grow with insufficient energy, obstructing the crystallization and resulting in an amorphous structure. This structure contains less grain boundaries and carriers are therefore less hindered, which increases the electrical mobility. This observation continues when the power goes down to 6%. Although the thickness is similar to that at 10%, the resistivity decreases further to 1.96 Ohm cm. The decrease in resistivity from 1 to 2 passes at 10% is due to the varying thickness having a considerable influence on the mobility of the carriers.

4.3.2   Transmittance

To get a full observation of the optoelectrical properties with changing the sputtering power, figure 4.15 shows the transmittance of the ZnO layer for these different recipes.
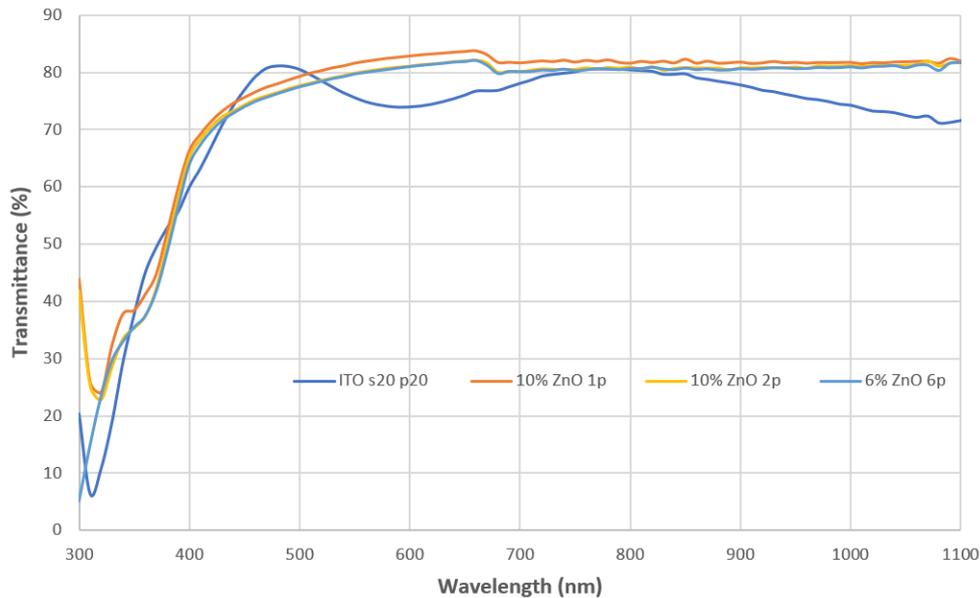
Figure 4.15: Transmittance in function of wavelength at different sputtering powers for ZnO

This plot shows that altering the sputter power does not influence the transmittance much. The transmittance curves at 10% (both 1 and 2 passes) and at 6% practically overlap. All the variations can be explained due to measurement errors. In comparison to the curve at 25%, the shapes differ somewhat, which is due to the thickness of the layer being 2.5 times larger. This is mainly caused by the difference of the interference within the ZnO layer. Here, it can be concluded that the sputtering power does not have an effect on the transmittance.

4.3.3 Solar performance

Similar to previous overviews of results, figure 4.16 provides the most important performance characteristics for the solar cells, the recipes of which are described in the table above.

Figure 4.16: Performance characteristics for different power recipes with corresponding amount of passes

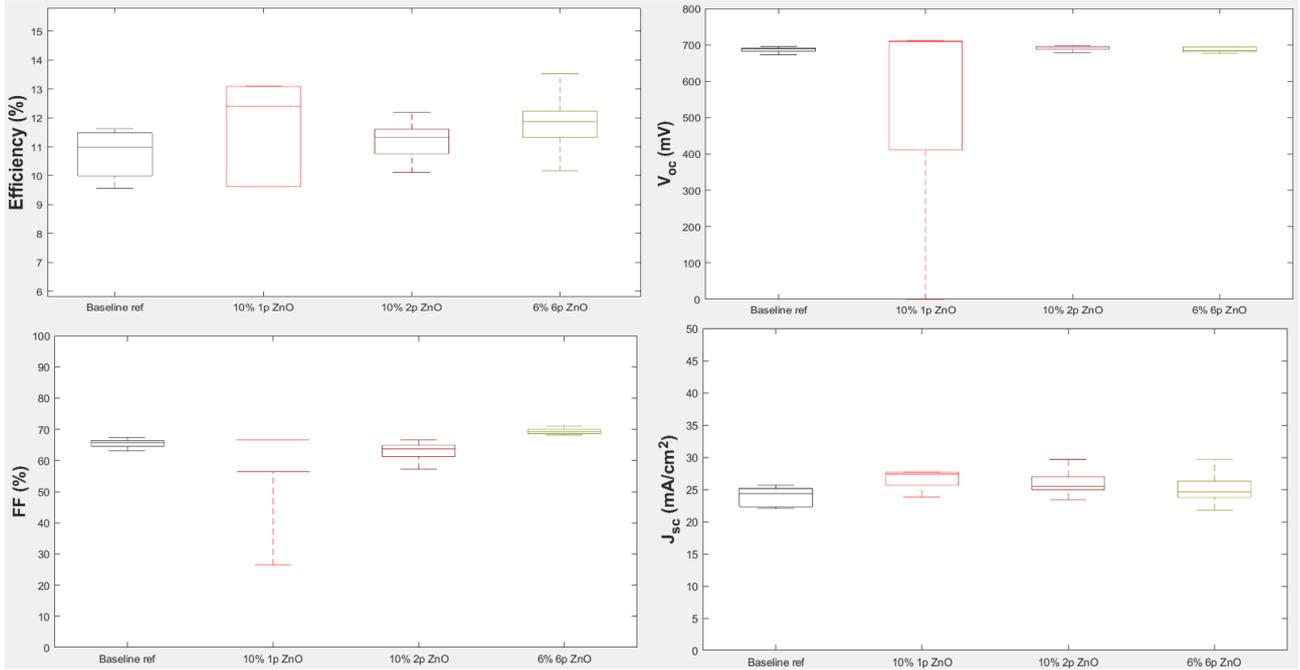By interpreting the general trend of the conversion efficiency, it can be said that this characteristic rises with decreasing power. Here its important to take both median and maximum efficiencies into account. To clarify the improvements, table 4.3 provides these values as a clarification of the boxplots.

Experiment	Baseline ref	10% 1 pass	10% 2 passes	6% 6 passes
Median efficiency (%)	10.97	12.40	11.32	11.78
Maximum efficiency (%)	11.62	13.10	12.20	13.80

Table 4.3: ZnO power changes overview of efficiencies

This table indicates that the maximum efficiency increases by about 2.2% and the median efficiency by about 1% when lowering the power to 6%. Another significant observation is that by adding another layer of ZnO with no additional oxygen gas, the spread on the values is lower. Which means that the cells are more similar and the improvement is more homogeneous. The open circuit voltage seems to be very similar. Important to take into consideration is that one faulty measurement of the voltage lead to an anomaly in the boxplot, which could not be detected during the experiment. The largest contribution to the efficiency can be seen in the positive trend of the fill factor. It rises from 65% to around 75%. The fill factor is an indicator of the concentration of defects which also causes the series resistance to increase, which is detrimental to the short circuit current density.

As mentioned before, the lower sputtering power directly causes the sputtered target particles to have less kinetic energy. This in turn reduces the amount of induced damage. Less atoms of the

underlying CdS and CIGS layers get displaced. Since the ZnO serves as a short circuit barrier [23], the lower sputtering creates less punctures where the generated electrons could directly recombine in the CIGS. This would cause less generated carriers to be transported to the grid. Another complementary theory is that the lower power creates surface that is less rough, which in turn mitigates the deterioration of the CdS/CIGS interface. A better surface quality also improves the further growth of the ITO which is deposited on top [22]. Overall, its the reduction in defects that directly translates to a performance increase.

A thorough discussion of these trends is provided in section 2.5.5. Studies show that increasing the thickness has a positive effect on all performance characteristics due to the reduced damage [10]. However, increasing the i-ZnO thickness even further resulted in a drop of the short circuit current density. They observed a conversion efficiency increase of 1.7% when increasing the thickness by 40 nm.

4.4   Time after CdS deposition

The fabrication of completed CIGS solar cells require many steps, each depositing a new layer or adding some feature. After the CIGS absorber layer has been selenized, the p-type buffer layer is realised trough a chemical reaction. At Energyville, Cadmium Sulfide (CdS) is chosen to be the buffer material. There are many parameters that influence the reaction process such as, but not limited to, temperature, Ph, reaction time and concentration. It has proven to be a process that is very sensitive to changing conditions. No two samples, even while undergoing a reaction with the same recipe, will have an identical CdS layer. Therefore, any measurements that are related to the quality of the CdS should be interpreted with caution. After the CdS reaction, the next layers to be added are the window layers (first ZnO and then ITO). It was speculated that waiting too long to start with the deposition of the window layers might be detrimental to the solar cell performance because of oxidation and other degradation phenomena. In addition, observing a dependency of waiting time on solar cell performance eliminates an unknown factor. This in turn acknowledges the reliability of the TCO optimization results.

To measure the influence of waiting time, two samples were created from the same CdS reaction batch. One got vacuum sealed right after the reaction, as to prohibit any continuous oxidation. This sample is equivalent to depositing the window layers immediately after the CdS reaction. The other one was not vacuum sealed and was stored in a box. A week later, both samples were used as substrates to sputter the ZnO, ITO and grids to form completed solar cells. Figure 4.17 provides the most important solar performance characteristics for both samples, in addition to the baseline reference, which was characterized in 4.1.4.
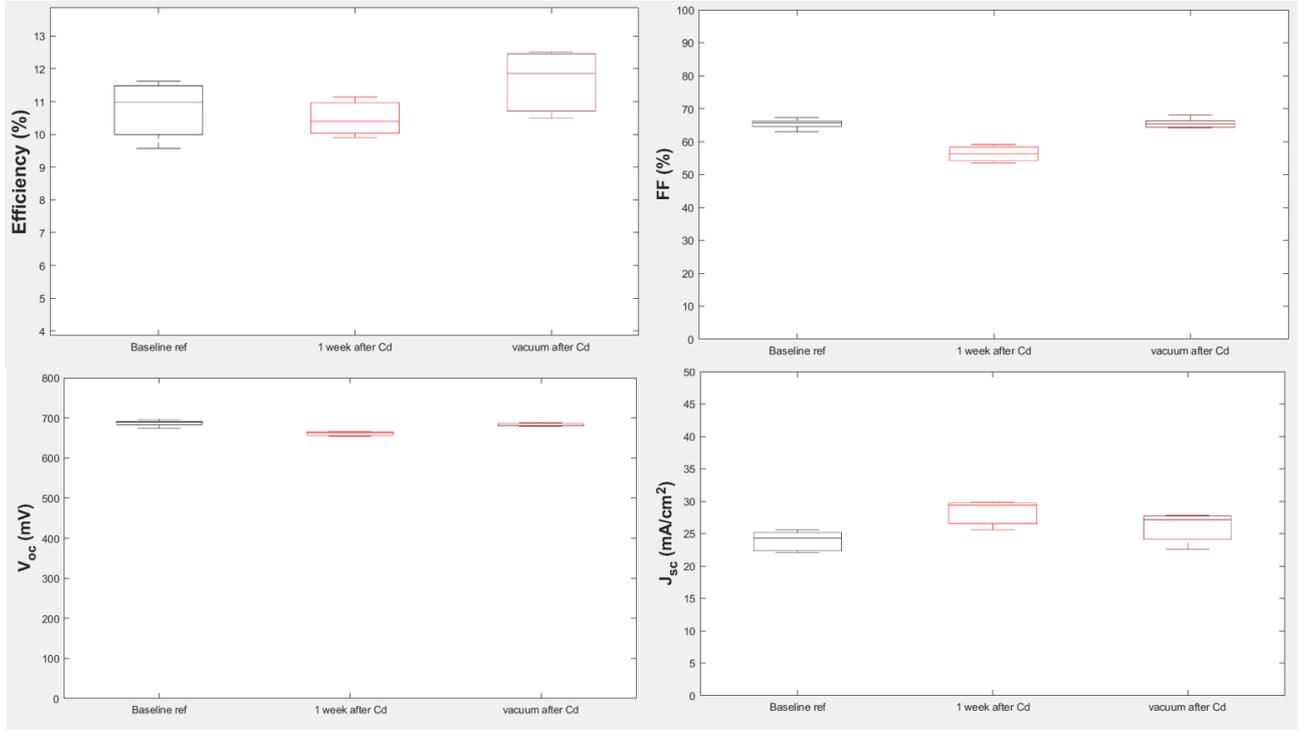
Figure 4.17: Performance characteristics for short and longer waiting time after CdS deposition to complete the solar cell

As can be seen in the upper left plot, the efficiency seems to be higher when the sample got vacuum sealed. In contrast, when storing the sample with an exposed CdS buffer, the completed cell seems to be less performing. The median difference of the conversion between the two waiting time extremes is 1.4%, which is quite significant. The vacuum sealed sample even performed better then the baseline reference (a median increase of 0.9%). This improvement is mainly due to the increase of the fill factor, which rises about 12% when comparing the 1 week waiting time with the vacuum seal. This might indicate that storing the sample in open air causes a certain oxidation of the CdS. This oxidation can block generated carriers from passing into the window layers, which adds a type of series resistance. This oxidation has the same effect as defects in the absorber layer, as discussed in previous sections.

4.5 Annealing of ITO

Annealing is commonly used to improve the transmittance and reduce the resistivity of TCO's. Therefore, it was of interest to use this technique to see if it is a viable optimization strategy for ITO. The samples used for the working pressure analysis were annealed at 200°C for 60 min. The middle samples were annealed with a gas flow of $10^3 \frac{Air^{-1n}}{h} N_2$, while the side samples were annealed in a pure O_2 environment. To not cause a thermal shock, the ramp down of the temperature after annealing was chosen to be three times slower.

Figure 4.18 plots the resistivity before and after annealing, in both O_2 and N_2 environments.

It is clear that after both O_2 and N_2 annealing, the resistivity drops by almost factor 3. It seems that the O_2 anneal was a little more effective, since at most pressures, the decrease is larger. An additional observation is that the small resistivity decrease when sputtering ITO at a higher working pressure has been canceled for both O_2 and N_2 annealing. The plots after annealing
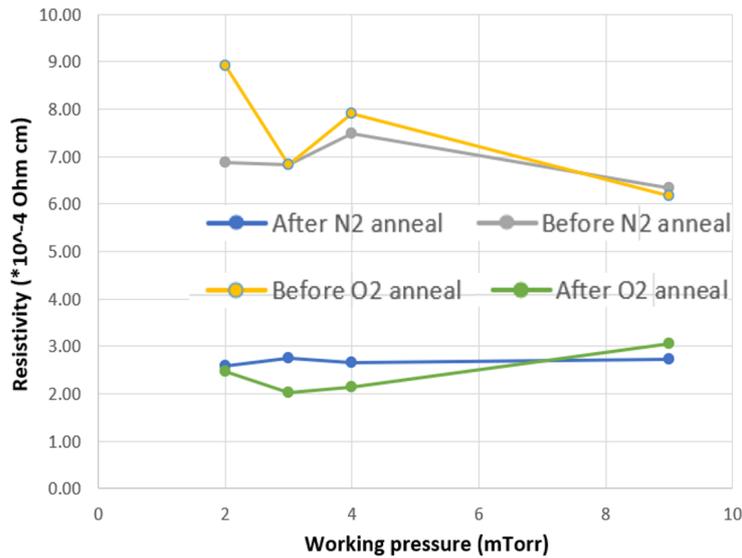
Figure 4.18: Resistivity of ITO before and after either O2 or N2 anneal at 200°C

seem to be practically flat.

To complete the optoelectrical analysis, the transmittance before and after annealing were measured for the same samples. Figure 4.19 plots a selection of the transmittance curves for both N_2 (left) and O_2 (right) annealing.
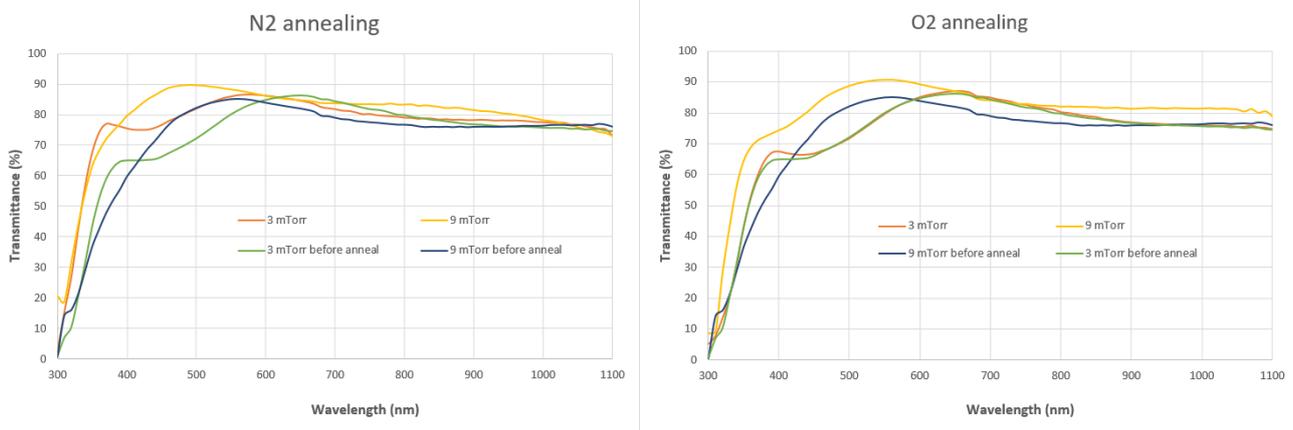

Figure 4.19: Transmittance in function of wavelength before and after N2 (left) and O2 annealing (right)

For the N_2 anneal, for both 3 and 9 mTorr, the transmittance increases significantly after annealing. The transmittance is elevated by around 10% at 480 nm and this rise is still visible at the longer wavelengths, where the difference gradually gets lower. Meanwhile for O_2 annealing, there is also a notable increase for the 9 mTorr sample. The transmittance is improved by 5% at 480 nm. This increase is practically consistent over the whole spectrum. However, annealing in O_2 did not affect the transmittance of the 3 mTorr ITO sample. These results might suggest another benefit of sputtering at a higher working pressure, being that annealing in both N_2 and O_2 environments is more effective in improving the transmittance.

The improvement of both optoelectrical properties can be explained because of an increase of both the carrier density and bandgap, as discussed in section 2.5.6 of the literature study. In essence,

the increased bandgap has to do with the Burstein-Mos shift as a result of a high concentration of free electrons. The crystallinity is improved, which in turn results in a lager grain size.

Chapter 5

Conclusion and outlook

For this thesis, the optoelectrical properties and the deposition mechanism of ITO and ZnO were optimized by investigating the effects of certain sputtering parameters. These parameters include the working pressure, the carrier speed and the sputtering power. Additionally, the effect of annealing and the waiting time after CdS deposition were examined. By depositing on SLG substrates, it was possible to measure the resistivity and optical properties such as transmittance, reflectance and absorbance. The new window layer recipes were also implemented to complete CIGS solar cells to achieve better performances.

A broader view at the overall properties of the current window layers indicates that the opto-electrical quality is already satisfactory. When all the optimizations are combined, the resistivity would only decrease slightly and the transmittance would not be affected much. This entails that the optoelectrical properties of the ITO and ZnO are able to compete with window layers realized by other research. The lowest achieved resistivity for ITO was $5.82 \cdot 10^{-4} \Omega cm$ and $2.03 \cdot 10^{-4} \Omega cm$ after O_2 annealing. The highest transmittance (that was not due to a reduction of the thickness) that was observed to be 87% at 500 nm. It is important to note that a higher working pressure did result in ZnO-films with a resistivity that was 3 order higher then at a low pressure. This surge is beneficial since the Zno functions as a short-circuit barrier. Varying the carrier speed did not have a beneficial effect on the optoelectrical properties of the TCO's and actually worsened the solar cell performance. Annealing the ITO samples resulted in a reduction of the resistivity by factor 3.

More importantly, altering the deposition mechanism resulted in significant improvements to the solar cells. This was done by increasing the sputtering pressure (9 mTorr) for all the window layers and decreasing the sputtering power (6%) for the initial i-ZnO layers. Both parameter adjustments resulted in a lower amount of damage to underlying layers. The higher pressure indirectly achieved a softer sputtering and filled oxygen vacancies, while the lower sputtering power directly mitigated defects to the CdS and absorber layers.

Now an overview of the achieved performance gains will be given. A first observation was that if the ZnO and ITO are deposited at 9 instead of 3 mTorr, the solar cells were more stable. This meant that after a month, the efficiency was barely affected while baseline samples lost up to 3% conversion efficiency. When depositing the window layers on a sample that was vacuum sealed right after the CdS reaction, an increase in efficiency from 11.5% to 12.5% was observed. When lowering the power of the initial ZnO passes, the performance is increased significantly. Instead

of 25% as is used in the baseline, sputtering at 10% increases the maximum achieved efficiency by from 11.6% to 13.1%. When the power is reduced even further to 6% and loss in deposition rate is compensated with extra passes, the maximum efficiency reaches a record 13.8%.

However, there are still some parameters that were left unchanged, which could be investigated in future research. One of these is the oxygen rate during the secondary ZnO layer deposition. Another interesting parameter could be the power of the ITO layer, which could result in better optoelectrical properties. Although the deposition time has been taken into consideration for this thesis, there are still experiments to be done around extending or perhaps shortening certain steps in the sputtering process. Additionally, the silver-nickel grid that comes on top of the window layers and the CdS buffer layer reaction still requires optimization.

References

[1] DS New Energy, "Cigs zonneceltechnologie," [online]. Available: https://nl.dsisolar.com/info/cigs-solar-cell-technology-32787367.html [Accessed: 12-04-2022].

[2] W. N. Shafarman and L. Stolt, *Cu(InGa)Se2 Solar Cells, chapter 13 in Handbook of Photovoltaic Science and Engineering*. Newark: Wiley, 2011.

[3] Matt Hughes, "What is rf sputtering?," [online]. Available: https://http://www.semicore.com/news/92-what-is-rf-sputtering [Accessed: 10-04-2022].

[4] T. Karasawa and Y. Miyata, "Electrical and optical properties of indium tin oxide thin films deposited on unheated substrates by d.c. reactive sputtering ," *Thin Solid Fimls*, vol. 223, pp. 135–139, 1993.

[5] Y.-S. Kim, "Influence of O2 admixture and sputtering pressure on the properties of ITO thin films deposited on PET substrate using RF reactive magnetron sputtering ," *Surface and Coatings Technology*, vol. 173, no. 2-3, pp. 299–308, 2003.

[6] M.-J. Zhao *et al.*, "Effect of working pressure on Sn/In composition and optoelectronic properties of ITO films prepared by high power impulse magnetron sputtering," *Vacuum*, vol. 196, 2022.

[7] M. H. Ahn, "Characteristics of ITO-resistive touch film deposited on a PET substrate by in-line DC magnetron sputtering," *Vacuum*, vol. 101, pp. 221–227, 2014.

[8] K.-S. Tseng and Y.-L. Lo, "Effect of sputtering parameters on optical and electrical properties of ITO films on PET substrates," *Applied Surface Science*, vol. 285, no. Part B, pp. 157–166, 2019.

[9] W.-S. Liu and H.-M. Cheng, "Indium tin oxide with titanium doping for transparent conductive film application on CIGS solar cells," *Applied Surface Science*, vol. 354, no. Part A, pp. 31–35, 2015.

[10] S. Almhammadi *et al.*, "Optimization of Intrinsic ZnO Thickness in Cu(In,Ga)Se2-Based Thin Film Solar Cells," *Materials*, vol. 12, no. 1365, 2005.

[11] J. L. Gray, *The physics of the solar cell, chapter 3 in Handbook of Photovoltaic Science and Engineering*. West Lafayette: Wiley, 2011.

[12] L. Alvarez-Fraga, "Indium-tin oxide thin films deposited at room temperature on glass and PET substrates: Optical and electrical properties variation with the H2–Ar sputtering gas mixture," *Applied Surface Science*, vol. 344, pp. 217–222, 2015.

[13] A. Klamchuen *et al.*, "Characterization of ITO thin films on PET substrates prepared by gas-timing RF magnetron sputtering," *e-Journal of Surface Science and Nanotechnology*, vol. 3, pp. 272–275, 2005.

[14] B. Yoo, "ITO/ATO/TiO2 triple-layered transparent conducting substrates for dye-sensitized solar cells," *Solar Energy Materials and Solar Cells*, vol. 92, no. 8, pp. 873–877, 2008.

[15] D. Kim, "Characterization of low pressure annealed ITO/Au/ITO films prepared by reactive magnetron sputtering," *Journal of Alloys and Compounds*, vol. 493, no. 1-2, pp. 208–211, 2010.

[16] W. K. A. Klöppel, "Dependence of the electrical and optical behaviour of ITO–silver–ITO multilayers on the silver properties," *Thin Solid Films*, vol. 365, no. 1, pp. 139–146, 2000.

[17] H. L. Yu Wen, "Transparent and conductive indium tin oxide/polyimide films prepared by high-temperature radio-frequency magnetron sputtering," *Journal of Applied Polymer Science*, vol. 132, no. 44, 2015.

[18] S. M. Diederik Depla, *Reactive Sputter Deposition*. Gent: Springer, 2008.

[19] D. M. Mattox, *The Foundations of Vacuum Coating Technology*. Oxford: William Andrew, 2018.

[20] K. F. Toshiro Maruyama, "Indium tin oxide thin films prepared by chemical vapour deposition," *Thin Solid Films*, vol. 203, no. 2, pp. 297–302, 1991.

[21] J. H. Kim, "Electrical, structural, and optical properties of ITO thin films prepared at room temperature by pulsed laser deposition," *Applied Surface Science*, vol. 252, no. 13, pp. 4834–4837, 2006.

[22] N. F. Cooray, "arge area ZnO films optimized for graded band-gap Cu(InGa)Se2-based thin-film mini-modules," *Solar Energy Materials and Solar Cells*, vol. 49, pp. 291–297, 1997.

[23] W. Gao, "ZnO thin films produced by magnetron sputtering," *Ceramics International*, vol. 30, no. 7, pp. 1155–1159, 2004.

[24] A. Chen *et al.*, "A new investigation of oxygen flow influence on ITO thin films by magnetron sputtering," *Solar Energy Materials and Solar Cells*, vol. 120, pp. 157–162, 2003.

[25] S. Yang and J. Zhong, "Influence of base pressure on property of sputtering deposited ITO film," *Journal of Materials Science: Materials in Electronics*, vol. 30, pp. 13005–13012, 2019.

[26] V. Teixeira *et al.*, "Amorphous ITO thin films prepared by DC sputtering for electrochromic application," *Thin Solid Films*, vol. 420-421, pp. 70–75, 2002.

[27] T. Sathiaraj, "Effect of annealing on the structural, optical and electrical properties of ITO films by RF sputtering under low vacuum level," *Microelectronics Journal*, vol. 39, no. 12, pp. 1444–1451, 2019.

[28] M. Medina-Montes *et al.*, "Effect of Sputtered ZnO Layers on Behavior of Thin-Film Transistors Deposited at Room Temperature in a Nonreactive Atmosphere," *Journal of Electronic Materials*, vol. 40, no. 6, pp. 1461–1469, 2011.

[29] H.-J. Yu *et al.*, "Light-soaking effects and capacitance profiling in Cu(In,Ga)Se2 thin-film solar cells with chemical-bath-deposited ZnS buffer layers," *Physical Chemistry Chemical Physics*, vol. 18, pp. 33211–33217, 2016.